



# Politecnico di Torino

Master's Degree in Aerospace Engineering  
Academic year 2023/2024

## Model for prediction of Hall-thrusters performance

Supervisor:  
Prof. Casalino Lorenzo

Candidate:  
Vigliotti Fabio

July 2024

*“There are no limits for a mind and a  
heart that will to succeed.*

*Anything is possible”.*  
**IRONMAN**

# Index

- Abstract**..... vi
- 1. Introduction** ..... 1
  - 1.1 Space propulsion** ..... 1
  - 1.2 Electric space propulsion**..... 4
    - 1.2.1 Electrothermal propulsion: resistojets and arcjets ..... 5
    - 1.2.2 Electrostatic propulsion: ions and Hall effect thrusters ..... 11
    - 1.2.3 Electromagnetic thrusters: SFMPD and PPT ..... 15
  - 1.3 Definitions and relations** ..... 19
  - 1.4 Efficiencies and performance** ..... 21
  - 1.5 Hall Thrusters** ..... 27
    - 1.5.1 Magnetic field generator ..... 30
    - 1.5.2 Ionization ..... 31
    - 1.5.3 Acceleration ..... 32
    - 1.5.4 Neutralization ..... 33
    - 1.5.5 Hollow cathode ..... 34
- 2. Mathematic model** ..... 41
  - 2.1 Introduction and assumptions** ..... 41
  - 2.2 Plasma generator** ..... 42
  - 2.3 Power losses** ..... 47
  - 2.4 Efficiency for Hall Thrusters** ..... 50
- 3. Results and applications** ..... 53
  - 3.1 Performance** ..... 54
  - 3.2 Advantages and limitations** ..... 55
  - 3.3 Applications** ..... 56
- 4. Bibliography and websites** ..... 57
- 5. Thanksgiving** ..... 58

## Figures index

Figure 1: Sketch of a vortex-heater resistojet .....	8
Figure 2: Sketch of a sealed-cavity resistojet.....	8
Figure 3: Picture of a resistojet thruster .....	9
Figure 4: Sketch of an arcjet thruster .....	10
Figure 5: Picture of an arcjet thruster.....	11
Figure 6: Sketch of an ion thruster.....	13
Figure 7: Sketch of a MPD thruster.....	16
Figure 8: Sketch of a PPT .....	17
Figure 9: Thrust vs Beam voltage .....	19
Figure 10: $I_{sp}$ vs Beam voltage .....	20
Figure 11: $I_{sp}$ vs $\eta_m$ @400 V .....	22
Figure 12: $I_{sp}$ vs $\eta_m$ @19 mg/s.....	22
Figure 13: $\gamma$ vs dts .....	24
Figure 14: $I_{sp}$ vs dts @400 V .....	24
Figure 15: $\eta_d$ vs $\eta_m$ .....	25
Figure 16: $\eta_e$ vs $\eta_m$ .....	26
Figure 17: $\eta_t$ vs dts.....	27
Figure 18: Sketch of a Hall Thruster .....	28
Figure 19: Sketch of a TAL .....	29
Figure 20: Magnetic field shape in NASA-173Mv.....	30
Figure 21: $I$ vs $V$ for different values of $B$ .....	31
Figure 22: Channel regions along the axis.....	31
Figure 23: Neutral density and ionization rate along channel axis.....	32
Figure 24: Electric field and voltage drop along the channel axis.....	33
Figure 25: Radial $B$ and axial $E$ along channel axis .....	33
Figure 26: Electrons' typical trajectory .....	34
Figure 27: Hollow cathode geometry .....	35
Figure 28: Hollow cathode regions .....	35
Figure 29: Cathode with keeper electrode .....	36
Figure 30: Different cathode shapes.....	36
Figure 31: Emission current density vs $T$ for different materials .....	38
Figure 32: Cathode channel erosion @30.000 hours.....	40
Figure 33: Cathode keeper erosion .....	40
Figure 34: Electrons and ions trajectory in an electro-magnetic field .....	43
Figure 35: Plasma sheath potential .....	44
Figure 36: Efficiencies vs discharge voltage .....	52
Figure 37: Picture of SPT-100 Hall Thruster .....	53

## Tables index

Table 1: Resistojets' characteristics .....	9
Table 2: Arcjets' characteristics .....	11
Table 3: Comparison between ion thrusters .....	12
Table 4: PPT performance .....	18
Table 5: Comparison between MPD and PPT .....	18
Table 6: Ion thruster vs Hall thruster performance .....	28
Table 7: Fitting coefficients for electrons emission .....	38
Table 8: Tabled SPT-100 data.....	54
Table 9: Data assumptions .....	54
Table 10: Model results.....	55

## Abstract

The purpose of this work is to build up a numerical model to study the performance of Hall thrusters with direct current discharge and dielectric walls, starting from their measurable data and quantities ( $V_b$ ,  $I_b$ ,  $P_{in}$ , etc). The model is almost ideal and considers just some of the total real losses (beam divergence, electrons wall losses, multiply charged ions, etc) since some phenomena (such as anomalous transport and secondary emission) are extremely challenging to be modelled. Plasma region is modelled with a steady-state 1-D model, considering ionization and acceleration effects together. Hollow cathode and its plasma are considered to be in stationary conditions as well. Afterwards all the models are linked together with the purpose of evaluating the overall performances and provide a sizing of the thruster. The Russian Hall Thruster SPT-100 is taken as a reference to use characteristics values (required power, thrust,  $I_{sp}$ , etc) and have realistic output and sizing. Optimum values are then compared to the real ones to evaluate the goodness of the model.

# 1. Introduction

Electric space propulsion has its roots in the 1960s, when especially Russia focused on this sector to gain dominance in the Cold War. Since the 1990s, knowledge and development of electric space propulsion has spread to the West as well, thanks to the strong growth of space industry and exploration. Electric thrusters have the advantage of being very versatile and can be used for both precision manoeuvres and AOCS, as well as for long interplanetary missions that require high-power thrusters. Their most advantageous aspect lies in the high specific impulse if compared to chemical propulsion, making them especially suitable for long missions that require a large  $\Delta V$ . In addition, a high specific impulse allows for reduced propellant consumption, increasing the available payload mass. The following work focuses on Hall-effect thrusters (named as Hall Thrusters or HT), a particular category of electrostatic thrusters, investigating the main aspects of their functioning in order to build a mathematical model to calculate their performance and efficiencies. For this, some pre-existing models will also be used, so as to highlight not only the advantages and limitations of these thrusters, but also the main mechanisms of power loss, in order to exclude small losses that, if taken into account, would increase the complexity of the calculation, but would not improve the quality of the model all that much.

## 1.1 Space propulsion

Space propulsion's history begins in the early 1900, with the first theoretical models developed in USA, Russian Federation and Europe by physicists and engineers such as Robert Hutchings Goddard, Konstantin Tsiolkovsky and Robert Esnault-Pelterie. It took just 20 years before the first flying rocket: in 1926 the American professor and scientist Robert Goddard built and flew the first liquid hydrogen rocket. Since then, the develop has been quite fast, especially during the Second World War and the Cold War, with a new boost in the latest years due to a renewed interest in space exploration and the advent of private companies working on it. Propulsion in space missions is essential to maintain and change the orbital parameters of a spacecraft and it is based on the same principle as the aeronautic propulsion: the third law of motion. In fact, all types of thrusters accelerate and eject a working fluid, so that the fluid itself pushes the spacecraft in the desired direction. Space propulsion can be divided into two main categories:

- chemical propulsion: the working fluid is obtained by a chemical reaction, which provides the energy required to generate thrust;
- electric propulsion: the working fluid is energized thanks to an external electric power source (typically a battery linked to solar panels).

To study the effects of ejecting fluid in space, it can be considered a 1-D problem and an isolated system, in which momentum is conserved:

$$m * V = (m - dm_p) * (V + dV) - dm_p * (c - V)$$

where  $m$  and  $V$  are respectively the spacecraft mass and speed before ejection,  $dV$  is the speed variation of the spacecraft due to ejection,  $dm_p$  is the ejected mass and  $c$  is the exhaust velocity of the ejected propellant. Ignoring the second order infinitesimal terms, the equation becomes:

$$m * dV = dm_p * c$$

Being  $\dot{m}_p = \frac{dm_p}{dt}$ , since propellant is continuously ejected, and  $T = \text{thrust}$ , it becomes:

$$m * \frac{dV}{dt} = \dot{m}_p * c = T$$

which is basically Newton second law, in the case of a non-constant mass. Also, the thrust power can be written as:

$$P_T = \frac{1}{2} \dot{m}_p c^2 = \frac{T * c}{2} = \frac{T^2}{2\dot{m}_p}$$

This means that, for a fixed required thrust, a lower exhaust velocity seems to be better since it requires less power, but on the other side this would lead to an increase in propellant consumption. Typically, a high exhaust velocity is preferable, as propellant mass reduction is much more critical than required power reduction in space missions. The overall effect of the thrust can be evaluated by the total impulse  $I_t$ , which is the total amount of impulse that the thruster can give to the spacecraft:

$$I_t = \int_{t_i}^{t_f} T dt$$

while the total required mass propellant  $m_p$  is:

$$m_p = \int_{t_i}^{t_f} \dot{m}_p dt$$

One of the most important parameters in space propulsion is specific impulse  $I_{sp}$ , measured in seconds, which represents the efficiency of propellant usage, regardless of the global effect measured by total impulse:

$$I_{sp} = \frac{I_t}{m_p g_0}$$

where  $g_0$  is the gravity acceleration at sea level. Considering thrust and fuel consumption as constants, specific impulse can be written as:

$$I_{sp} = \frac{c}{g_0}$$



and it can be intended as how long the thruster can provide thrust equal to the weight of the propellant. This means that a higher specific impulse leads to a lower propellant mass required for the mission, with all the consequent benefits for the mission design.

The link between the mission design and the propulsion system is represented by  $\Delta V$ , the total change in speed that the thruster must be able to provide to the spacecraft during the mission. The total propellant mass can be derived from  $\Delta V$  as follows:

$$\Delta V = \int_{t_i}^{t_f} \frac{T}{m} dt = \int_{t_i}^{t_f} \frac{\dot{m}_p \cdot c}{m} dt = -c \cdot \int_{m_i}^{m_f} \frac{dm}{m}$$

being  $\dot{m}_p = -\frac{dm}{dt}$ . Solving the integral yields the rocket equation, also known as Tsiolkovsky equation:

$$\frac{m_f}{m_i} = e^{-\frac{\Delta V}{c}}$$

Thus, the required propellant mass  $m_p$  will be:

$$m_p = m_i - m_f = m_i(1 - e^{-\frac{\Delta V}{c}})$$

It means that, for a fixed  $c$ , the propellant mass will grow exponentially with respect to  $\Delta V$  while, for a fixed  $\Delta V$ ,  $c$  and  $\Delta V$  should be comparable in order to have an acceptable propellant (thus payload) mass. The final spacecraft mass  $m_f$  is sometimes called as delivered mass ( $m_d$ ), since it represents the net mass that can be pushed to the end of the mission, using all the available propellant. It is important to notice that  $m_d$  includes not only the useful mass (also known as payload mass), but also all subsystems mass (structure, power system, thermal control system, etc).

One of the main differences between chemical and electric propulsion is the typical value of  $c$ , that is about 2-7 km/s for chemical thrusters and 5-100 km/s for electric thrusters. Therefore, chemical thrusters are suitable for short mission, in which a low  $\Delta V$  is required, while electric propulsion should be used in long missions, that require a huge  $\Delta V$ . The other very different aspect is thrust-to-weight ratio, which is hundreds to millions times bigger in chemical reactors than in electric thrusters: once again it can be noticed that chemical propulsion is suitable for short missions with high thrust required, while electric propulsion is better for long missions, in which propellant saving is crucial. Typically, chemical and electric propulsion are coupled in long missions, since the electric propulsion can't provide high thrust values: a chemical rocket is use in the first phase of the mission, where high thrust is required, while an electric thruster is used outside of the atmosphere, where low thrust is sufficient, to minimize the propellant mass.

## 1.2 Electric space propulsion

Electric space propulsion can be divided into 3 main categories, depending on how electric power is used:

- electrothermal propulsion: the propellant is heated by electric energy and then expanded in a nozzle;
- electrostatic propulsion: the propellant is ionized and then accelerated by an electrostatic field;
- electromagnetic propulsion: the propellant is ionized and then accelerated by a combination of electric and magnetic fields.

In electric propulsion, a power source is mandatory since the propellant itself can't provide any amount of energy. The most common solution is a battery, integrated on the spacecraft with solar panels that can recharge the battery after it's been discharged and while it's used. Other solutions, such as nuclear power, are possible but not yet developed. Based on the design power, electric thrusters can be used for precision manoeuvring ( $P_E \approx 1 W$ ), orbit insertion ( $P_E \approx 1 kW - 100 kW$ ) and human space missions ( $P_E \approx 100 kW - 1000 kW$ ). As will be shown, despite the wide power range, electric propulsion provides so small thrust that it can only be used in space, where gravity forces are almost completely balanced by centrifugal forces and aerodynamic forces are irrelevant. Since electric power  $P_E$  is provided by an external source, it is independent from  $\dot{m}_p$  and they can be regulated separately to obtain different values of  $c$  (or  $I_{sp}$ ).

The balance between input and output power is:

$$\dot{m}_p \cdot \left( h_c + \frac{v_{ex}^2}{2} - h_0 \right) = \eta P_E$$

$$P_T = \eta P_E = P_E - losses$$

where  $h$  and  $v_{ex}$  are respectively specific enthalpy and exit velocity of propellant and  $\eta$  is the total thruster efficiency. Therefore, the exit velocity can be written as:

$$v_{ex} = \sqrt{\frac{2\eta P_E}{\dot{m}_p}}$$

which can be considered equal to  $c$  in the ideal case. So it is:

$$T = \dot{m}_p \cdot v_{ex} \rightarrow P_T = \frac{T \cdot v_{ex}}{2} = \eta \cdot P_E$$

$$v_{ex} = \frac{2\eta P_E}{T}$$

Therefore  $v_{ex}$  can be increased by increasing  $P_E$  or reducing  $\dot{m}_p$ . It must be considered that increasing  $P_E$  requires an increase in the power source mass  $m_s$  as well. Being  $\alpha$  the proportional factor between power source mass and power supplied ( $m_s = \alpha P_E$ ) the acceleration provided to the spacecraft is computed as:

$$\alpha = \frac{T}{m} < \frac{T}{m_s} = \frac{T}{\alpha P_E} = \frac{T}{\alpha \frac{T \cdot v_{ex}}{2\eta}} = \frac{2\eta}{\alpha \cdot v_{ex}}$$

For typical values of  $\eta$ ,  $\alpha$  and  $v_{ex}$  (respectively 0,5, 10 kg/kW and 10 km/s) the resulting acceleration is a millesimal fraction of  $g_0$ , which states that electric thrusters can only be used in space as mentioned. The best advantages in electric thrusters are specific impulse, propellant consumption and range of power. In fact, due to the high  $v_{ex}$  that can be reached, specific impulse has a typical value of 1500-4000 s, about 5 to 10 times greater than typical values of  $I_{sp}$  in chemical propulsion. A direct consequence of high  $I_{sp}$  is a strong reduction in propellant mass required for a given mission. On the other side, electrical propulsion can provide only small thrust in the order of units to hundreds of  $mN$  and, due to instabilities in involved phenomena (especially plasma instability), thrust can't be regulated all that much. Some principal solutions for electric propulsion will be shown below.

### 1.2.1 Electrothermal propulsion: resistojets and arcjets

Electrothermal propulsion is based on propellant heating to produce thrust. In particular, the idea is to make propellant evaporate thanks to an electric power source and let it expand in a nozzle. The main solutions, sufficiently popular to date, are resistojets and arcjets. The former make use of an electrical resistance, of appropriate geometry, to deposit heat into the propellant via the Joule effect, while the latter originate with the idea of being able to reach much higher temperatures in the propellant by depositing energy into it through the creation of an electric arc (hence their name). The following will list the main relationships useful in assessing performance and losses of these thrusters.

Firstly, it is important to define the electrical power needed to heat the propellant, neglecting any losses at this stage. The assumption is that the final temperature  $T_c$  is much higher than the initial one (about 2000-3000 K) and therefore  $T_c - T_i \approx T_c$ . The electric power needed will then be:

$$P_E \approx \dot{m}_p C_p T_c$$

where  $C_p$  is the propellant specific heat capacity.

Once  $T_f$  is defined, it is possible to evaluate the exhaust velocity using energy conservation. All flow losses will be ignored, so the exhaust velocity here described is an ideal one.

$$u_{id} = \sqrt{2C_p T_c}$$

At last, the ideal thrust  $T_{id}$  can be computed as:

$$T_{id} = \dot{m}_p u_{id}$$

Some considerations can be made about this category of thrusters. The most important aspect is the maximum temperature that can be reached: both power and thrust are directly dependent on this parameter and it seems to be preferable to have the highest possible temperature. However, rising temperature leads to a number of critical issues:

- Materials: a higher working temperature is possible only if walls are made up of a heat-resistant material, otherwise material properties limit maximum temperature;
- Power: rising temperature requires more power, which sometimes can be difficult to provide and manage;
- Losses: a higher temperature leads to higher losses due to radiation, dissipation and dissociation/ionization, so an accurate trade-off must be done;
- Life: thruster life mainly depends on its erosion due to oxidation, particle bombardment and creep, and rising temperature accelerates all these processes.

The second consideration is about the propellant choice. In this simple model, power, thrust and exhaust velocity are related to  $C_p$ , which should be as high as possible. This suggests that low atomic mass propellants would be preferable, but in reality there is a trade-off due to storage, dissociation and erosion issues (especially if liquid  $H_2$  is considered as a propellant). The most used propellants are liquid hydrogen, ammonia and hydrazine. The first one has the lowest atomic mass of any propellants, but presents dissociation (and recombination with other elements) problems, which can accelerate the erosion rate of the thruster. Storage is also critical, as it must be stored as a liquid, which requires extremely low temperatures and high pressure. Ammonia ( $NH_3$ ) still has a low atomic mass, especially after dissociation, but its best side is that it's easy to store and manage, solving many of the problems one has to deal with when using hydrogen. Its weak point regards frozen flow loss: in fact, after dissociation occurs, a large amount of energy is not recovered, producing quite high frozen flow losses. At last, hydrazine ( $N_2H_4$ ) is similar to ammonia, since it is easy to store, it has low atomic mass after dissociation and presents frozen flow losses as downside. However, the best upside about hydrazine is that its dissociation is exothermic: once the thruster is turned on, it can provide thrust even in the case of an electric system failure or breakdown.

At this point, it is important to mention that pulsed devices such as Microwave Thrusters and Laser Sustained Plasma Thrusters fall into this propulsion category as well, but they won't be described in detail. The main idea behind their functioning is to use extremely high-power currents (in the order of MW), tuning them in order to avoid high temperature issues and limitations.

## Losses

Resistojets and arcjets have three main losses mechanisms: thermal losses, frozen flow losses and aerodynamic losses:

Thermal losses are all kind of losses due to heat exchange and high temperatures management. In fact, due to high temperatures, radiated power from walls cannot be neglected, as well as power dissipation from propellant to walls. This loss mechanism is quite easy to manage, since a good insulating system, together with a proper material choice and a good spacecraft design can limit the majority of heat losses. It is also important to manage heat fluxes in order to avoid erosion and unnecessary thruster degradation, which is the main limit to thruster life. The most critical parameter of thermal losses is the high temperature needed to increase thruster performance, and thermal efficiency of the thruster can be evaluated as:

$$\eta_{th} = \frac{\dot{m}_p C_p T_c}{P_e}$$

Frozen flow losses are the most difficult to manage, since they are probabilistic and have chemical origins. Frozen flow losses represent all the energy that is 'frozen' in the exhaust flow due to propellant dissociation and ionization. This energy can't be recovered because it can't be converted into kinetic energy of the flow, and because of these losses, the thrust is reduced because the exhaust velocity is lower than expected in the ideal case. Frozen flow efficiency is defined as follows:

$$\eta_{ff} = \frac{u_e^2}{2C_p T_c}$$

The last main power loss mechanism is aerodynamic loss. Actually, this loss is due to the non-uniform outlet flow, which can diverge and have different local velocities along its section. Taking into account this loss requires at least a 2-D flow model, because 1-D is not sufficient to point out all phenomena that must be considered. This mechanism has a direct impact on thrust, which is reduced even in the case of an ideal exit velocity. Aerodynamic efficiency can be described as:

$$\eta_{ae} = \frac{P_{thrust,real}}{P_{thrust,ideal}} = \frac{T \cdot c}{\dot{m}_p u_e^2} = \frac{c^2}{u_e^2}$$

being  $c$  the effective exhaust velocity.

## Resistojets

As mentioned before, resistojets use a resistor to heat and vaporise the propellant, but this process can be achieved in two different ways. The older concept was to use a vortex heater, so that an efficient heat exchange between resistor and propellant is promoted due to a high contact surface between them. In this way, the critical aspect is resistor erosion due to propellant dissociation and chemical reactions: material choice and temperature managing are essential to ensure a sufficient efficiency of the thruster during all its life. On the other hand, the new concept is a sealed cavity: a resistor is enclosed in a sealed cavity to avoid direct contact with propellant, and heat transfer is achieved by radiation of the cavity towards the outside. This solves most erosion problems, but a higher resistor temperature is required together with an efficient radiation mechanism, otherwise efficiency and thrust won't be so great to justify the complexity of a sealed cavity instead of a vortex heater.

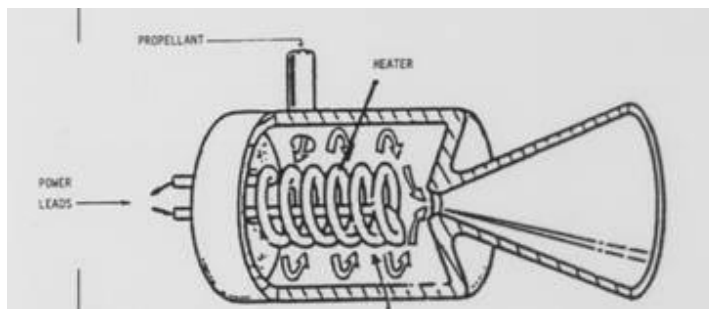


Figure 1: Sketch of a vortex-heater resistojet

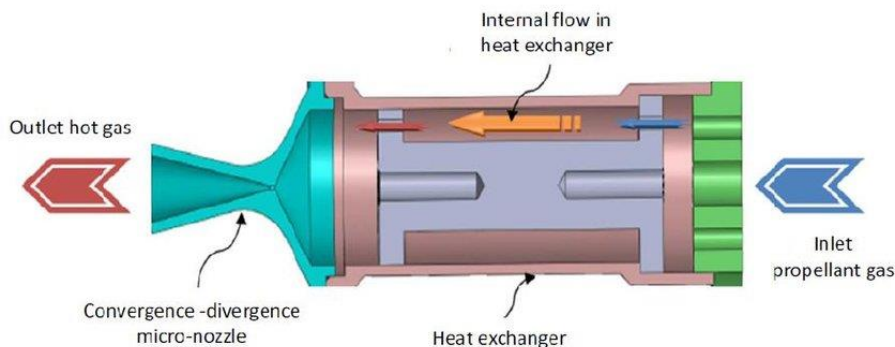


Figure 2: Sketch of a sealed-cavity resistojet

One of the best aspects of these thrusters is that they don't need a specific voltage or current to work properly (as usually happens with ions and Hall effect thrusters): this implies that they can use the same voltage produced by solar arrays. This solution almost avoids the need for a Power Processing Unit (PPU), thus reducing weight, costs and complexity.

On the other hand, the most demanding aspects of resistojets design are about heat management and dissociation. In fact, it is essential to provide the thruster with appropriate heat shields, so that thermal losses are as low as possible and efficiency is improved. It is possible to reduce heat loss with a passive system (insulating and low emitting materials) or an active system (heat transfer, refrigerator) which uses a small amount of electric power to reduce overall heat emission. Dissociation is the last loss mechanism that must be properly treated, but in the majority of cases it is sufficient to raise chamber pressure (up to 1-20 atm) in order to limit as much as possible dissociation rates. Nowadays, resistojets are mostly used in station keeping, with an average power of about 1 kW.

**Resistojets: Characteristics and Performance**

propellant	N <sub>2</sub> H <sub>4</sub>	NH <sub>3</sub>
<i>I<sub>sp</sub></i> , s	300	350
<i>P<sub>E</sub></i> , W	500-1500	500
<i>η</i>	0.8	0.8
voltage	28	28
thruster mass, kg/kW	1-2	1-2
PPU mass, kg/kW	1	1
feed system	blowdown	regulated
lifetime, h	500	-
missions	SK, insertion, deorbit	orbit corrections

*Table 1: Resistojets' characteristics*

In the table above, the principal resistojets characteristics are summarized, while a real resistojet thruster can be seen in the picture below.

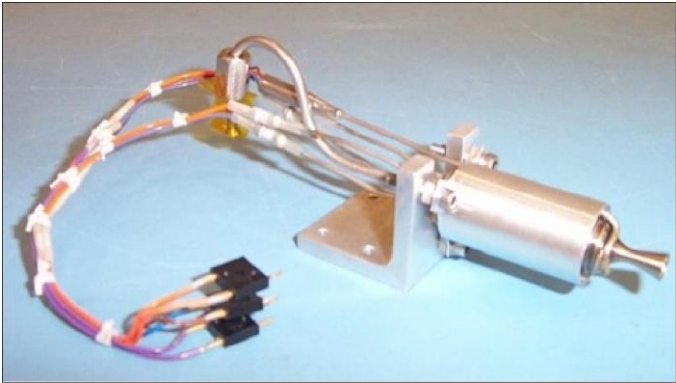


*Figure 3: Picture of a resistojet thruster*

## Arcjets

This category of thruster represents a sort of evolution of resistojets, in an attempt to overcome materials limits and increase  $T_c$ . In fact, arcjets don't have a resistor but uses the propellant itself as a resistor: a small plasma region is created between the cathode and the anode, ionizing propellant via electron bombardment. Once the plasma is created, an arc between cathode and anode occurs and a high current flows in it, depositing a huge amount of heat in propellant thanks to the Joule effect. In this way, there is no direct contact between propellant and resistor and  $T_c$  can be raised up to 10.000 K. Obviously this is a local temperature, since thruster walls couldn't resist to such high temperatures: all around the arc, a propellant vortex is created in order to shield walls. In the figure below, a sketch of arcjet's design is shown.

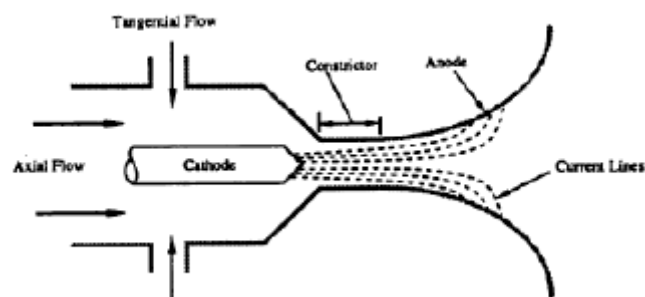


Figure 4: Sketch of an arcjet thruster

The typical cylindrical geometry can be observed: the inner cathode provides electron emission to create plasma, while a coaxial outer anode collects electrons to maintain a sufficient plasma current to provide Joule heating. The most used solution for cathode to emit electrons is thermionic mechanism, although sometimes field effects can be used as well (a better study of the emitting cathode will be presented later). Propellant flow has both axial and tangential velocity components to promote a good wall insulation, as mentioned above.

As one can imagine, the presence of the plasma implicates a series of downsides to deal with. First of all, the arc in the plasma interacts with its magnetic field creating the so called 'pinch effect', which is basically a self-constriction of the arc. An external magnetic field can be applied to reduce this effect, but it must be mentioned that the swirling vortex created to prevent walls from too high temperatures is helpful for pinch effect as well. Also, the arc presents many instabilities, both in low and high frequencies, making it difficult to manage and control it. The last difficult aspect of using plasma is about PPU: in fact, plasma needs a negative volt/ampere input characteristic to be stabilized. This makes the PPU design extremely demanding, and the PPU itself is typically much heavier than others used in other kinds of thrusters. Other key issues, such as frozen flow losses, electrode erosion and thermal losses are important as well, but they are typically managed in a very similar way as in resistojets, so they won't be illustrated here.



The current arcjet employment is station keeping in GEO satellites, requiring a power close to 1 kW, while a 30 kW arcjet thruster is studied for future orbit insertions. The main arcjets characteristics are resumed in the table below, together with a picture of a real arcjet thruster.

**Arcjets: Characteristics and Performance**

propellant	N <sub>2</sub> H <sub>4</sub>	NH <sub>3</sub>	H <sub>2</sub>
$I_{sp}$ , s	500-600	500-800	1000
$P_E$ , W	300-2000	500-30k	5k-100k
$\eta$	0.35	0.3	0.4
voltage	100	100	200
thruster mass, kg/kW	0.7	0.7	0.5
PPU mass, kg/kW	2.5	2.5	2.5
feed system	regulated	regulated	regulated
lifetime, h	1000	1500	-
missions	SK	SK, orbit raising	medium $\Delta V$ transfers

*Table 2: Arcjets' characteristics*



*Figure 5: Picture of an arcjet thruster*

### 1.2.2 Electrostatic propulsion: ions and Hall effect thrusters

Electrostatic propulsion includes all kinds of thrusters that use an electric field to produce thrust. In this category, the most important thrusters are Ions Thruster (IT) and Hall effect Thruster (HT), even though less popular solutions (such as Field Effect Electric Propulsion and Colloidal Thrusters) are sometimes used especially when extremely high specific impulse ( $\sim 6000$  s) is required (at the price of an extremely low thrust,  $T \sim \text{few } \mu\text{N}$ ). In this section, only ions thrusters are described, since Hall Thrusters will be treated more accurately in the next chapters. Ion thrusters present a typical cylindrical geometry and their functioning is based on three main phases: ionization of the propellant, acceleration of the ions and neutralization of the exit beam.

In fact, propellant is injected in the chamber, where an emitting cathode provides a huge number of electrons. During their path to the anode, electrons collide with propellant atoms, ionizing them if their collision is sufficiently energetic. This mechanism leads to a plasma creation in the chamber, made up by emitted electrons, secondary electrons (those removed from propellant atoms when ionization occurs), positive propellant ions and neutral propellant atoms (other species, such as double-ionized ions and walls emitted electrons are present as well, but will be neglected in this description). Once ions are created, their acceleration is essential to generate thrust: this is achieved using two grids, screen grid and acceleration grid, located at the exit of the chamber, with an extremely high electric field between them. In this way, if positive potential grid (screen grid) is the inner one, ions are extracted from plasma and accelerated toward the outer space, thus generating thrust. Finally, neutralisation is essential to maintain the charge neutrality of the spacecraft. This is provided by a second, smaller cathode, located outside the chamber, which is responsible for emitting an electron current equal to the ion current to neutralise the beam. It is important to notice that this emission creates an almost negligible thrust, since electrons have a very small mass if compared to ions mass, and also a low energy level (thus low exit speed) in order to minimize power losses. At this point, it is clear that plasma creation is the basis of the functioning of the thrusters: this is the reason why a magnetic field is essential to ensure a good efficiency. In fact, a radial magnetic field is always created in the chamber, in order to limit electrons mobility towards the anode and extend as much as possible their residence time in the chamber. By doing so, collision probability between electrons and neutral propellant atoms is raised as much as possible, reducing losses due to emitted electrons that are collected by the anode before a collision occurs. Typically, a permanent magnet (or more than one) is used to create a magnetic field, but other solutions based on current coils are possible as well. A sketch of Ions Thruster geometry, together with some typical values of their performance, is shown below.

## Ion Thrusters Comparison

Name	XIPS 13	XIPS 25	NSTAR	RITA 15	RITA 150	T5	T6
Builder	Hughes (Boeing)	Hughes (Boeing)	Hughes (Boeing)	Astrium	Astrium	Quinetiq	Quinetiq
$P$ , kW	0.33	4.5	0.5-2.3	0.5	4.3(1-6)	0.27-0.65	5.2
$I_{sp}$ , s	2570	3800	3100	3-5000	3-5000	3-3500	3500
$T$ , mN	18	165	20-95	15	150	10-25	40-200
$\eta$	0.7	0.7	0.63			0.64-0.66	
$D$ , cm	13	25	30	10	22	10	22

*Table 3: Comparison between ion thrusters*

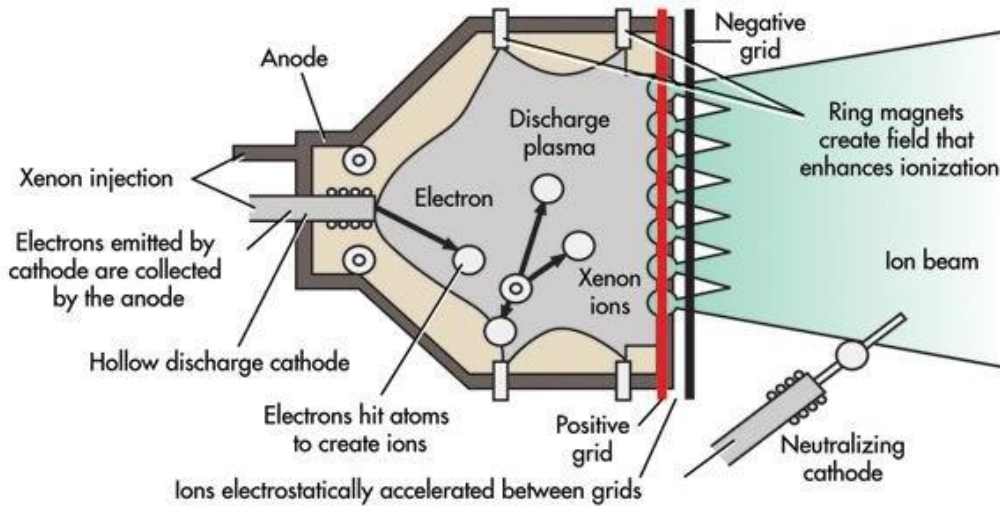


Figure 6: Sketch of an ion thruster

The main assumption made to simplify the study of Ions Thruster is that all the thrust is created by ions acceleration, neglecting both electrons and neutral atoms that escape from the chamber or that are emitted by neutralizer cathode. Under this assumption, the exit velocity is calculated using energy conservation:

$$u_+ = \sqrt{\frac{2qV_N}{M_+}}$$

where  $u_+$  is ion exit velocity,  $V_N$  is the net accelerating potential,  $M_+$  is the ion mass and  $q$  is the ion charge (equal to  $e$  if double ionization is neglected). Then propellant consumption is computed as:

$$\dot{m}_p \approx \dot{m}_+ = \frac{I \cdot M}{q}$$

where  $I$  is the ejected ion current and  $M$  is propellant atomic mass (supposed equal to  $M_+$ ).

Since ionization power represents one of the main power losses, it is essential to promote ionization as much as possible in order to increase the efficiency. This is achieved by a set of expedients about chamber parameters and their regulation. In particular, it is necessary to have a low pressure, low density and low ions density plasma in the chamber. Low pressure (typical values are about  $10^{-5}$  torr) is useful to confine plasma and neutral propellant, avoiding its premature escape from the chamber without being ionized, while low ions density (usually plasma is made up by 10% ions + 90% neutral atoms) keeps the probability of useful collisions high and reduces the probability of double ionization. It also helps in reducing ionization cost, because if ions density grows too much, then it is more difficult to further ionize propellant and a higher electron emission, together with a higher emitted electron energy, would be required. As mentioned, the magnetic field and its shape and intensity are crucial in ionization as well. In the further description, plasma will be assumed to be quasi-neutral (electron density  $n_e$  almost equal to ion density  $n_i$ ) and all of its species are assumed to have a Maxwellian energy distribution. Due to ion acceleration

and emission, it is clear that recombination between them and emitted electrons in the plume region is almost impossible and it can't provide any amount of recovered energy: once again it points out the importance of reducing as much as possible ionization power. An ideal efficiency can be calculated, considering ionization as the only power loss mechanism:

$$\eta_{id} = \frac{\frac{m_+ u_+^2}{2}}{\frac{m_+ u_+^2}{2} + \epsilon_b}$$

which is the ratio between the thrust power and the input power, being  $\frac{m_+ u_+^2}{2}$  the kinetic energy of emitted ions and  $\epsilon_b$  the energy spent for ionization. It is important to mention that electrons are emitted from the cathode with an energy level  $\epsilon_b > \epsilon_i$  (being  $\epsilon_i$  the minimum energy required for ionization) in order to increase the probability of an ionizing collision between emitted electrons and neutral atoms. This parameter also takes into account the amount of electrons that go to the anode without ionizing collisions. For xenon, the most common propellant,  $\epsilon_i = 12,13 \text{ eV}$  while  $\epsilon_b \approx 30 \text{ eV}$ . It can be noticed that ideal efficiency grows for higher atomic mass, higher exit velocity (thus higher specific impulse) and lower ionization cost.

For what concerns acceleration, it is important to understand the mechanism that leads to its limitation. In fact, once a large number of ions enter the gap between the accelerating grids, it becomes more difficult to squeeze more ions into that region and accelerate them. Also, electric field and potential profile change their values, up to the extreme condition in which electric field changes its sign, degrading completely thruster performance. The maximum current value between the grids is stated by Child-Langmuir law:

$$J_{max} = \frac{4\epsilon_0}{9} \left( \frac{2q}{m_+} \right)^{\frac{1}{2}} \cdot \frac{V_G^{\frac{3}{2}}}{x_a^2}$$

where  $J_{max}$  is the maximum current density,  $\epsilon_0$  is vacuum dielectric constant,  $V_G$  is the potential between the grids and  $x_a$  is the distance between the grids. This law represents the main limit to thrust density, since it directly depends on emitted current, and it states that it is necessary to build a bigger thruster (so that they have a bigger exit area) if a higher thrust is required.

In ions thrusters, neutralization is essential not only to ensure spacecraft charge neutrality, but also to prevent ions back streaming. In fact, once they are emitted, the ions find themselves between the accelerating grid behind them (charged to a negative potential) and the previously emitted ions in front of them (which creates a positive potential zone). This configuration, if not properly managed, can lead to ions flowing back towards the thruster, nullifying thrust and degrading efficiency. The solution is to emit neutralizing electrons as close as possible to the accelerator grid, so that the

beam is quasi-neutral as well and ions do not experience any potential drop in the beam. Child's law limits electron emission as well, but this limit is overcome by emitting plasma instead of single electrons, in which a much higher current can flow.

To complete the overview on ion thrusters, it is essential to mention that few models use radiofrequency radiation to ionize propellant, but aside from this difference, their functioning is completely equal to the ones described. Also, the cathode is a crucial component of the thruster, but it will be described in detail in the HT section.

Nowadays, Ion Thrusters are used for station keeping purposes and primary propulsion in interplanetary flights.

### 1.2.3 Electromagnetic thrusters: SFMPD and PPT

Electromagnetic thrusters (EMT) represent the most advanced technological concept in space propulsion, but due to the issues related to their functioning they have been used almost only in experimental flights, without a real large-scale diffusion. Their functioning is based on plasma creation and ions acceleration as electric thrusters do, with the substantial difference that in EMT the electric field is used for plasma creation while magnetic field is responsible for ions acceleration to create thrust. The best advantages related to these thrusters regards thrust and specific impulse. In fact, thanks to the high-current level, these thrusters can produce high thrust values, which makes them suitable for interplanetary missions. On the other hand, the high power required (typically tens to hundreds of kW) is often a limit, due to the limited available power on the spacecraft. This could be overcome thanks to nuclear propulsion, which would provide extremely high-power levels without the need of a huge mass. Unfortunately, such technology is unavailable nowadays. Also, high power together with low efficiency generates thermal control and electrode erosion issues, which can be barely overcome using pulsed power and current. The last downside is their low electromagnetic compatibility: in fact, the high (eventually pulsed) current generates a strong electromagnetic interaction with the spacecraft, so a proper shield is necessary to avoid spacecraft damaging.

#### **SFMPD**

Self-Field MagnetoPlasmaDynamic (SFMPD) thrusters present a geometry similar to arcjets, in which an inner cathode generates a current through the plasma towards the anode walls. A tangential magnetic field is created by this current, and that field interacts with the current itself, pushing it toward the exit to generate thrust. It is also possible a quite different configuration, called Applied-Field MagnetoPlasmaDynamic (AFMPD), in which an external magnetic field generator is used to create the same pushing effect. Its functioning is almost equal to SFMPD, so it won't be described in detail, but the best advantage of such configuration is that magnetic field is independent from the flowing current, making it easier to control and regulate this type of thrusters.

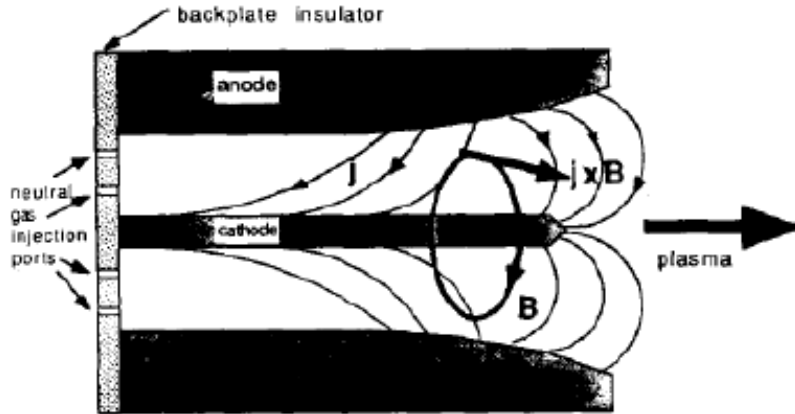


Figure 7: Sketch of a MPD thruster

Once this current-magnetic field configuration is created, two forces are created into the plasma, called blowing force and pumping force. The first one occurs due to interaction between radial current and tangential magnetic field. Its direction will be axial, toward the exit, so it will directly provide thrust. The second one instead is the interaction force between axial current and tangential magnetic field, and it is directed toward the channel axis. It creates a pumping effect, increasing local plasma pressure in the cathode zone. This change in pressure indirectly creates thrust thanks to the inner cathode. SFMPD's main performance parameter can be calculated as follows:

$$\text{Maecker equation: } T = J^2 \frac{\mu_0}{4\pi} \left( \ln \left( \frac{r_a}{r_c} \right) + 0,75 \right)$$

$$\text{Exhaust velocity: } c = \frac{T}{\dot{m}_p} \propto \frac{J^2}{\dot{m}_p}$$

$$\text{Input power: } P_T = \frac{T \cdot c}{2} \propto \frac{J^4}{\dot{m}_p}$$

where  $J$  is the current flowing into the plasma,  $r_a$  and  $r_c$  are respectively anode and cathode radius and  $\mu_0$  is vacuum magnetic permeability. It is clear that current is the most important parameter involved in performance computation, together with thruster geometry. The typical loss mechanisms can be grouped into the same previously described: thermal loss, frozen flow loss and aerodynamic loss. The first one occurs at the anode, due to the high current collection, and it is responsible for anode erosion as well, likely to what happens with arcjets. Its typical values can vary in a wide range, from 20% up to 80% of the total input power. The second one occurs in plasma, due to the necessary ionization process and due to the plasma instability. Depending on the flowing current, these losses are about 10% to 40% of the total power input. The last one occurs due to beam divergence, as happens for all the other electric thrusters, and typically represents about 10% of the total input power. From these numbers, it is possible to see how efficiency can be quite low in some configurations, which is a critical issue due to the high power required by these thrusters for the reasons discussed earlier.

## PPT

Pulsed Plasma Thruster represents an attempt to overcome the main MPD thrusters' limits. The idea they are based on is to use short current pulses at extremely high-current values (typically few MW of power and more than  $10^4$  A current). In this way, it is possible to have a high power avoiding most of thermal issues, thanks to the intermittent 0 A current in the duty cycle that allows an extended time range for the thermal control system to dissipate heat. The typical PPT configuration is shown in the next figure.

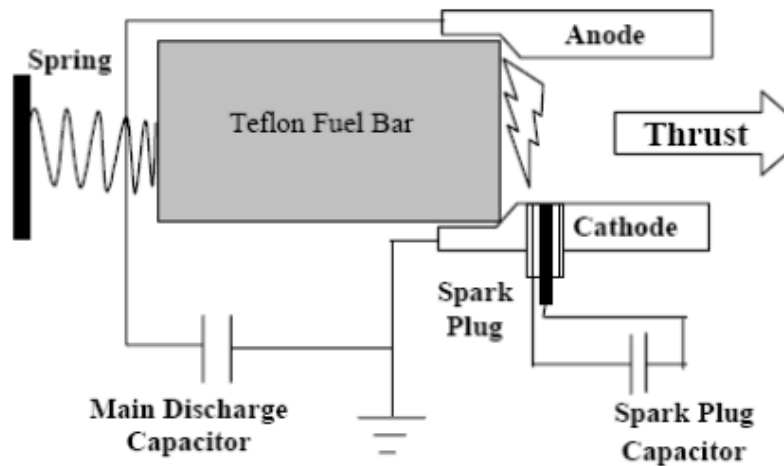


Figure 8: Sketch of a PPT

The most important difference between the PPT and the previously discussed electromagnetic thrusters is that they use solid propellant (Teflon fuel bar in the picture). The reason behind this choice is that a liquid propellant would require a pumps and valves system to be fed into the discharge chamber, but the reactivity of such system would be totally inadequate to execute the designed duty cycle due to the extremely short pulses (in the order of  $10 \mu\text{s}$ ). Instead, solid propellant can be evaporated and ionized thanks to the spark plug, located between the end of the fuel bar and the discharge chamber. In this way, the feeding electrical system is able to execute the duty cycle and provide a proper functioning of the thruster. Once a small amount of Teflon is evaporated and ionized, plasma is created, allowing the discharge current to flow from cathode to anode and generating the magnetic force that provides thrust, as previously described. The most important key issues for this thrusters category is the electromagnetic interference with spacecraft and low efficiency for the same reasons discussed in the SFMPD section. Also, it must be considered capacitors lifetime, which represents a limit to thruster lifetime, due to the high currents and powers they have to withstand. The next tables offer an overview of main PPT performances, together with a comparison between them and MPD.

## PPT: Characteristics and Performance

Thruster	$W_0$ J	$m_f/W_0$ $\mu\text{g}/\text{J}$	$I_{sp}$ s
LES-6	1.85	4.8	300
SMS	8.4	3.4	450
LES-8/9	20	1.5	1000
TIP-II (Nova)	20	2.3	850
MIT Lab	20	2.8	600
MIPD-3	100	2.0	1130
Millipound	750	2.5	1210
Primex-NASA	43	1.5	1136
IL PPT-3 Lab	7.5	10	600
Japan Lab	30.4	3.7	423
China Lab	23.9	1.9	990

Table 4: PPT performance

## Electromagnetic Thrusters: Characteristics and Performance

Type	PPT	AF-MPD	SF-MPD
$I_{sp}$ , s	500-1000	2000-5000	2000-5000
$P_E$ , W	1-200	1k-100k	200k-4M
$\eta$	0.1	0.5	0.3
voltage, V	1000-2000	200	100
thruster mass, kg/kW	120	?	?
PPU mass, kg/kW	100	?	?
lifetime	$10^7$ pulse	?	?
$I_t$ , Ns	4000	-	-
missions	precise corrections	large- $\Delta V$ (med- $P_E$ )	large- $\Delta V$ (large- $P_E$ )

Table 5: Comparison between MPD and PPT



### 1.3 Definitions and relations

It is now important to re-define some typical space propulsion parameters in the case of electric propulsion, so that they can be computed easily starting from electrical thruster values.

The first consideration to be made is that thrust is given essentially by the ion beam, neglecting electron current. In fact, ions have a much greater mass, so for a fixed input power they will provide a much higher thrust than electrons since  $P$  is proportional to  $\dot{m}v_{ex}^2$  while  $T$  is proportional to  $\dot{m}v_{ex}$ . For this reason, it will be  $v_{ex} = v_{ions}$ , and, being  $M$  the ion mass, it can be computed by conservation of energy:

$$v_{ex} = \sqrt{\frac{2qV_b}{M}}$$

Once  $v_{ex}$  is defined,  $T$  and  $I_{sp}$  can be derived by their definitions. Considering  $\dot{m}_p = \dot{m}_i = \frac{I_b M}{q}$ , their expressions will be:

$$T_{ideal} = \dot{m}_p v_{ex} = \sqrt{\frac{2M}{e}} I_b \sqrt{V_b}$$

$$I_{sp} = \frac{T}{g_0 \dot{m}_p} = \frac{\sqrt{2eV_b}}{g_0 \sqrt{M}}$$

In the graphics above, it is shown the trend of  $T$ , for different fixed power levels as the beam voltage changes, and  $I_{sp}$  as beam voltage changes. From now on, ion mass is supposed to be Xenon ion mass ( $M = 2,18 \cdot 10^{-25} \text{ kg}$ ).

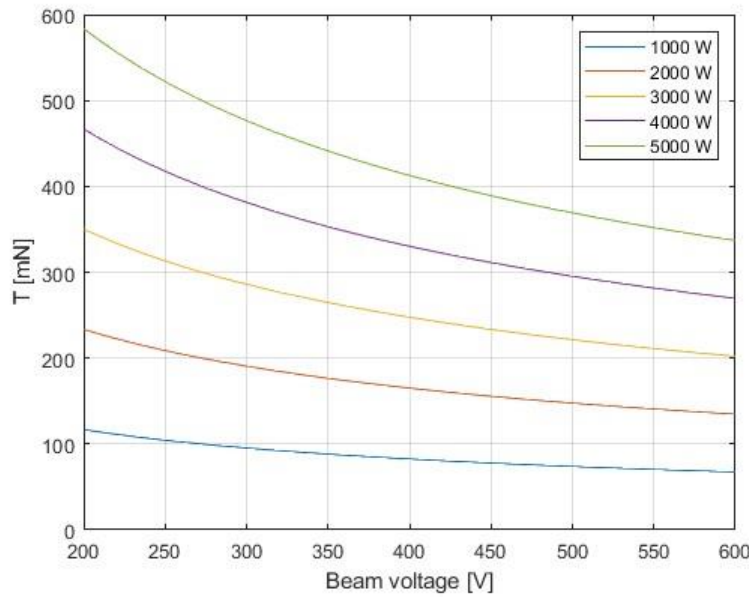


Figure 9: Thrust vs Beam voltage

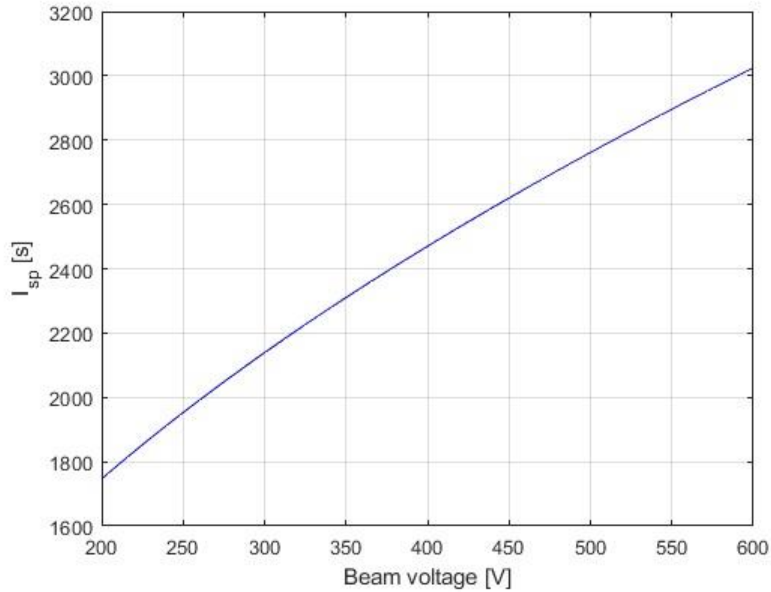


Figure 10:  $I_{sp}$  vs Beam voltage

What emerges from these graphs is that thrust and specific impulse are inversely related to beam voltage: in fact, increasing beam voltage leads to a thrust reduction (due to current reduction if the power is fixed) but also to a specific impulse improvement, since it is strictly dependent on exit velocity (thus beam voltage). A trade-off is necessary to choose the proper beam voltage value, depending on mission requirements. Also, power level does not affect specific impulse in this first approximation, since it depends only on beam voltage regardless of beam current.

The last useful parameter to describe the efficiency of the thruster is the Thrust-to-Power ratio, by now computed neglecting electrical loss (so  $P_{in} = P_{beam}$ ):

$$\frac{T}{P_{in}} = \frac{2}{g \cdot I_{sp}}$$

It is important to notice that ion mass is strictly related to thruster performance. For fixed beam current and voltage, a higher mass increases thrust and thrust-to-power ratio, at the cost of decreasing specific impulse. Also, it must be considered that a different ion mass (thus different propellant) would have an impact on mission costs and thruster testing: by now the most common propellant is xenon, but other possibilities are tested (krypton, argon, liquid bismuth and mercury). On the other hand, for a fixed power input, a high current seems to be better than a high voltage to improve thrust, but this would lead to higher plasma and electrical losses as will be shown, so a trade-off is essential for these variables.

## 1.4 Efficiencies and performance

In this section there will be a description of the main efficiencies used in the presented model to evaluate losses, considering different power loss mechanisms. It must be mentioned that the following are just 'model efficiencies' and they will be re-defined in the HT study in chapter 2 to have a more precise and accurate model.

### Mass utilization efficiency

This parameter is important to determine how well the propellant is ionized and expelled, since it considers the ionized propellant versus unionized propellant. Its definition in the ideal case is:

$$\eta_m = \frac{I_b \cdot M}{e \cdot \dot{m}_p}$$

which is basically the ratio between the expelled ion mass and the unionized propellant throughput. The mass utilization efficiency is directly involved in  $I_{sp}$  computation as follows:

$$I_{sp} = \frac{v_{ex}}{g} = \frac{v_i \dot{m}_i}{g \dot{m}_p}$$

$$T = \dot{m}_i v_i = \sqrt{\frac{2M}{e}} I_b \sqrt{V_b}$$

So it is:

$$I_{sp} = \frac{\eta_m}{g} \sqrt{\frac{2eV_b}{M}}$$

Once  $V_b$  is fixed, the  $I_{sp}$  is directly proportional to  $\eta_m$  while, for a fixed power level,  $I_{sp}$  decreases for growing  $\eta_m$  because an increase in ionization rate leads to a higher accelerated mass, thus a smaller  $v_{ex}$ . These relations are shown in the graphics below, considering realistic values of beam voltage and fuel consumption to give an example (respectively 400 V and 19 mg/s).

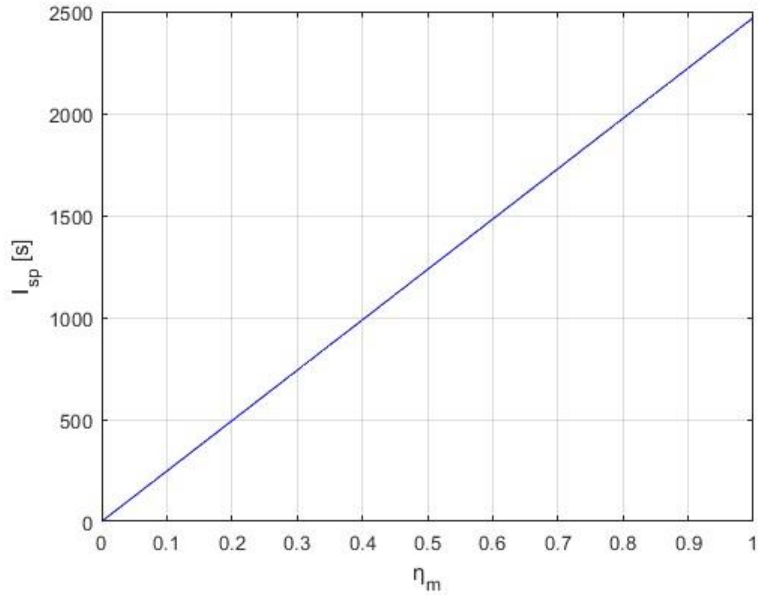


Figure 11:  $I_{sp}$  vs  $\eta_m$  @400 V

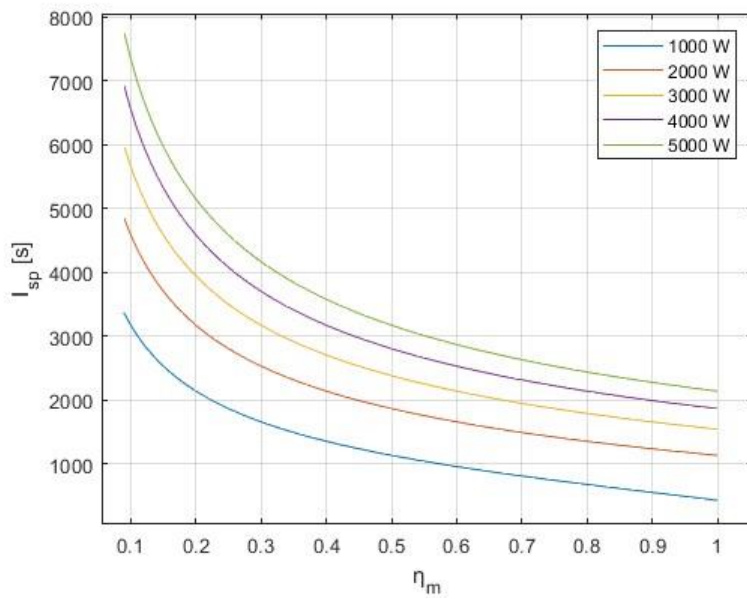


Figure 12:  $I_{sp}$  vs  $\eta_m$  @19 mg/s

In the real case, mass utilization efficiency should be corrected considering double ions. It is useful to define double-to-single ( $dts$ ) ion ratio as  $dts = \frac{I^{++}}{I^+}$ , and the correction factor will be:

$$\alpha_m = \frac{1 + \frac{1}{2}dts}{1 + dts}$$

The real mass utilization efficiency then is:

$$\eta_{m\_real} = \alpha_m \eta_{m\_ideal}$$

Typical values of  $dts$  are  $0,05 \div 0,2$ , leading to a correction factor of  $0,917 \div 0,976$  and  $\eta_{m\_real}$  values around  $0,85 \div 0,92$ .

### Thrust correction

This parameter is used to take into account beam divergence and double ionization thrust losses. The first factor to be considered is the average half-angle divergence of the beam  $\theta$ , that, in the ideal case of a constant ion current density, will reduce axial thrust of a factor:

$$F_T = \cos(\theta)$$

In Hall Thrusters, typical values of  $\theta$  are about 10-25 degrees, leading to some integration issues to avoid beam interaction with the spacecraft. In the case of a different current density distribution, this factor could easily be calculated by integrating the local divergence loss over the radius.

Considering also double ionization, the second correction factor will be similar to the one used for mass efficiency:

$$\alpha_T = \frac{1 + \frac{1}{\sqrt{2}} dts}{1 + dts}$$

It is important to notice that, for the same values of  $dts$  considered previously,  $\alpha_T$  assumes values of  $0,951 \div 0,986$ . This means that eventual double ionizations lead to a thrust reduction smaller than mass efficiency reduction.

The thrust correction factor  $\gamma$  will be:

$$\gamma = \alpha_T \cdot F_T$$

leading to a real thrust computed as:

$$T_{real} = \gamma \cdot T_{ideal}$$

The next graphic shows how  $\gamma$  changes for different beam divergence semi-angles and  $dts$ .

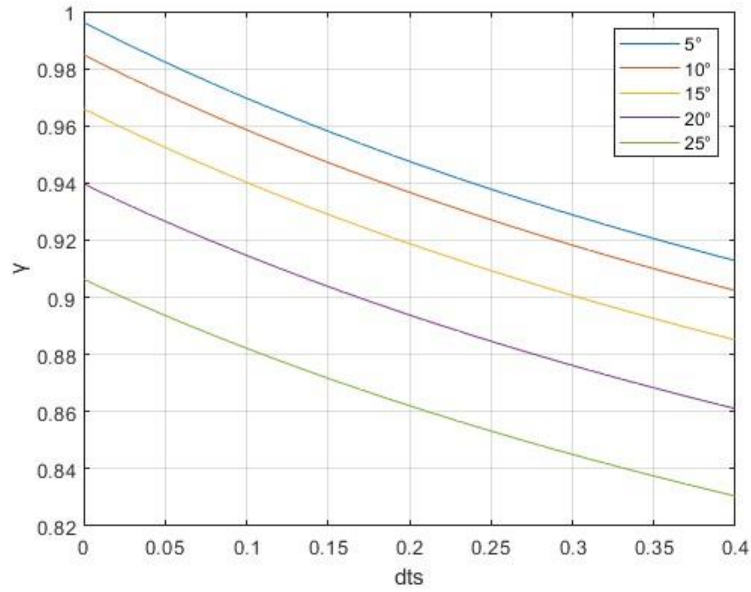


Figure 13:  $\gamma$  vs  $dts$

Typical values of  $\gamma$  in HT are  $0,90 \div 0,92$ , and thrust correction factor reduces  $I_{sp}$  as follows:

$$I_{sp} = \frac{T}{\dot{m}_p \cdot g} = \frac{\gamma \cdot \eta_m}{g} \sqrt{\frac{2eV_b}{M}}$$

In the following graphic, it is possible to observe  $I_{sp}$  trend with respect to  $dts$ , at a fixed beam voltage, while  $\eta_m$  is supposed to be constant and equal to 0,88.

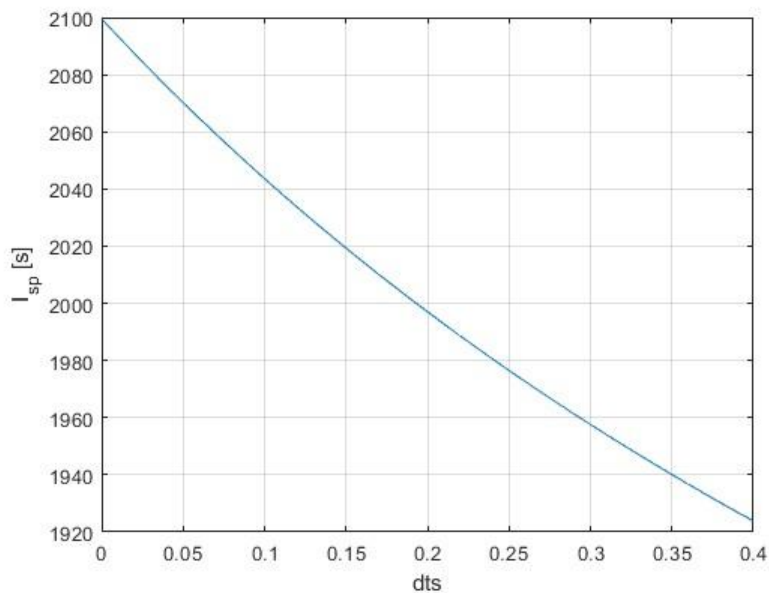


Figure 14:  $I_{sp}$  vs  $dts$  @ 400 V

## Electrical efficiency

The electrical efficiency is essential to consider the cost of ion beam production. In fact, this parameter is defined as the ratio between the beam power and the total input power:

$$\eta_e = \frac{I_b V_b}{I_b V_b + P_0}$$

where  $I_b V_b$  is the beam output power, while  $P_0$  represents all the other power input necessary to create the beam, such as electrical ionization power and cathode heater and keeper power. The other parameter closely related to electrical efficiency is the ion production efficiency  $\eta_d$ , which is the ratio of the power (discharge power) required to produce ions and the beam current.

$$\eta_d = \frac{P_d}{I_b} \left[ \frac{W}{A} \text{ or } eV/ion \right]$$

In contrast with all the other efficiencies, this parameter should be as small as possible, since it represents a power loss. Typical values of  $\eta_d$  in Hall thrusters are of a few hundreds of eV / ion. Discharge losses are related to mass utilization efficiency as shown in figure:

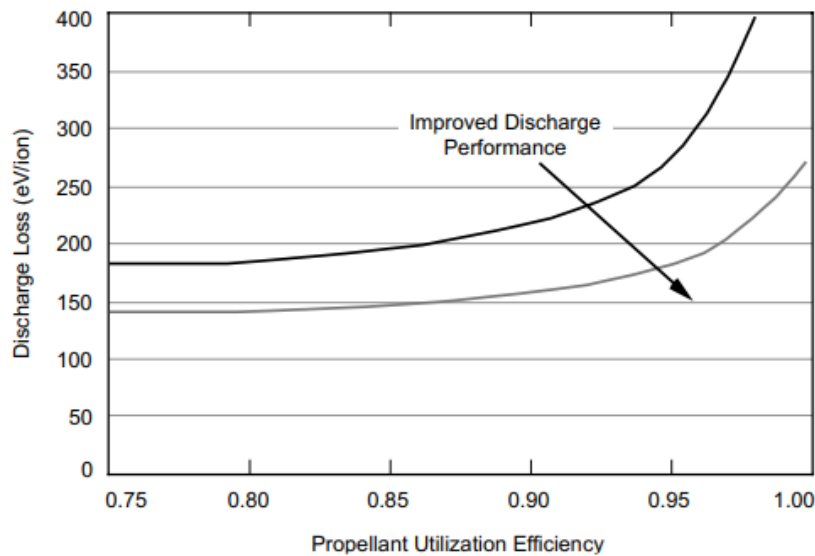


Figure 15:  $\eta_d$  vs  $\eta_m$

The mechanism that leads to an increase in discharge loss as mass efficiency increases is regulated by neutral plasma pressure. In fact, for a low mass efficiency, the neutral pressure in the thruster is high and the electron temperature is low. As mass efficiency increases, the neutral pressure decreases and the electron temperature raises, increasing discharge loss. The best trade-off is to operate the thruster near the knee of the curve, such that mass efficiency is high but discharge loss is still not excessive. In particular, this trend leads to an inverse proportionality between mass efficiency and electrical efficiency: as  $\eta_m$  approaches its maximum values,  $\eta_e$  rapidly decreases due to the increasing power required to ionize all the propellant. On the other side, for low values of  $\eta_m$ , the required ionizing power falls to much lower values,

leading to  $\eta_e$  values closer to 1. The typical trend between  $\eta_e$  and  $\eta_m$  is shown in the next graphic.

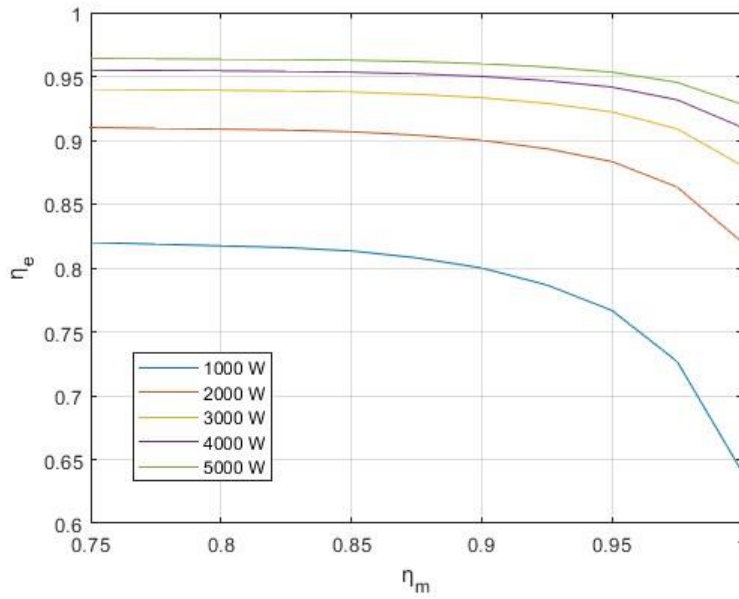


Figure 16:  $\eta_e$  vs  $\eta_m$

## Total efficiency

Total efficiency is the most general efficiency that can be defined, since it is the ratio between the output power and the input power, including all types of losses:

$$\eta_t = \frac{P_{jet}}{P_{in}} = \frac{T^2}{2\dot{m}_p P_{in}}$$

where input power is considered as the total power supplied by the power source. This parameter is extremely important especially for Hall thrusters, because it can be evaluated from easily measurable parameters during the tests in vacuum system, while other parameters used to calculate other specific efficiencies are more difficult to be measured precisely ( $I_b$ ,  $V_b$ ,  $v_{ex}$ , etc). Total efficiency is dependent on all the other efficiencies previously described, as it is the product between all of them. In fact, in its definition,  $T$  and  $P_{in}$  can be substituted with  $T = \gamma \sqrt{\frac{2M}{e}} I_b \sqrt{V_b}$  and  $P_{in} = \frac{P_b}{\eta_e} = \frac{P_{jet}}{\eta_e}$ , leading to total efficiency main definition:

$$\eta_t = \gamma^2 \eta_m \eta_e$$



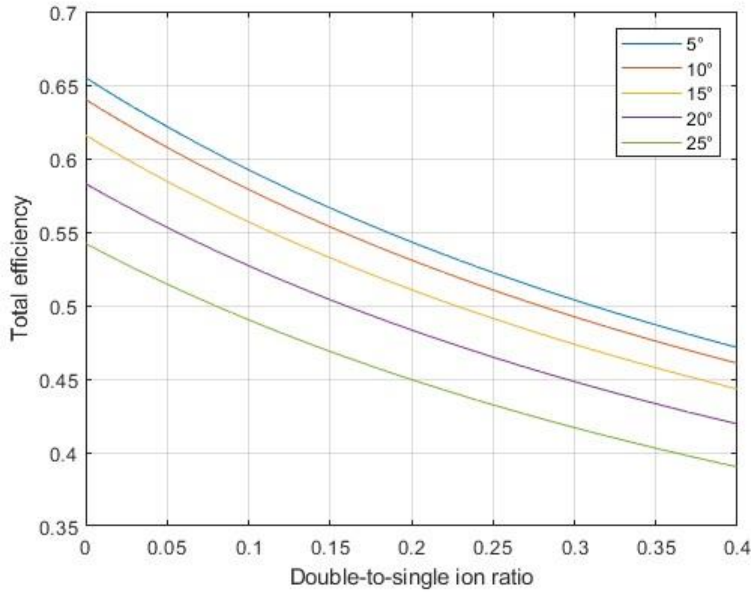


Figure 17:  $\eta_t$  vs  $dts$

In the graphic above it is shown  $\eta_t$  trend with respect to  $dts$  for different semi-divergence angles. Typical and constant values for  $\eta_m$  and  $\eta_e$  have been considered (respectively 0,88 and 0,75).

## 1.5 Hall Thrusters

As mentioned, Hall thrusters (together with ion thrusters) are the most common in electric space propulsion. The idea they are based on is to form a plasma in the ‘combustion’ chamber and then accelerate plasma ions outside the chamber to create thrust. In this way, Child-Langmuir law does not affect the maximum beam current, since the absence of the grids avoids space-charge limitations. That’s the reason why Hall Thrusters present much greater beam currents than Ion Thruster, at a lower voltage due to power limitations. Based on what was described above, considering the same power level, Hall Thruster typically will have higher thrust than Ion Thruster (due to higher beam current), but lowest specific impulse (due to lowest beam voltage): therefore, they will be chosen for shorter missions to avoid a too low payload mass. Hall thrusters have a typical cylindrical geometry, in which an annular anode and a cylindrical channel form the ‘combustion’ chamber. Almost all the propellant is injected near the anode and it is ionized via electron bombardment to create the plasma. An external cathode emits electrons, which flow into a plasma created using a small fraction of propellant, that are attracted by the anode at the end of the chamber. However, their mobility is reduced thanks to a radial magnetic field created by permanent magnets or current coils in the channel. Magnetic field is essential to provide a good efficiency of the thruster: in fact, its role is to keep electrons ‘orbiting’ in the channel as long as possible, in order to maximize the collision rate with propellant neutral atoms and ionize them. Once ions are created, the plasma itself, together with the electric field produced by the anode, accelerates them towards the channel exit, thanks to a huge potential drop near the exit. This mechanism will be discussed later

on. One particular characteristic of HT is that they don't need a neutralizer cathode, as other electrostatic thrusters do: in fact, the emitting cathode provides neutralization by emitting an electron current in the ion beam, thus spacecraft charge neutrality is assured. Even though a magnetic field is involved in HT, they are still considered electrostatic thrusters, since the magnetic field only keeps electrons in the chamber but it isn't directly involved in thrust creation.

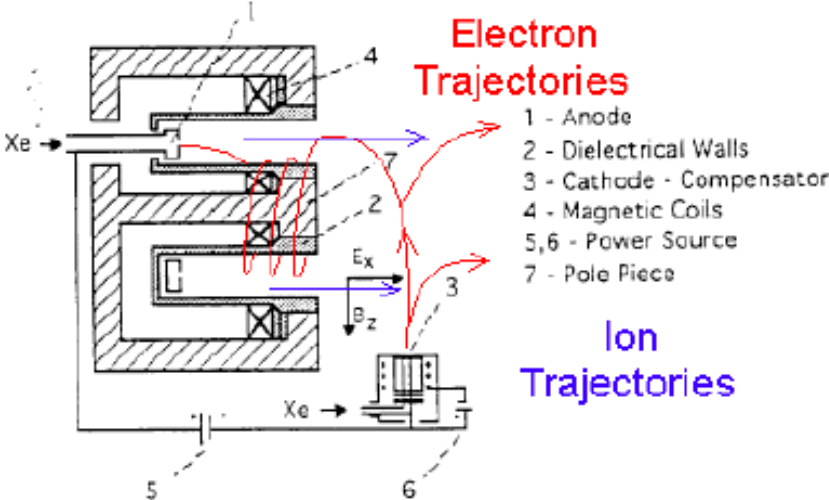


Figure 18: Sketch of a Hall Thruster

In the figure above, it is possible to see the typical cylindric geometry of Hall Thrusters: propellant is injected into the annular region where ionization occurs, while the anode provides the axial electric field to accelerate ions toward the exit. Simplified ion and electron trajectories are shown as well: as will be further described, electrons orbit in the annular channel and travel many orbits before reaching anode, while ions are almost undisturbed by the magnetic field due to their high mass. The table below lists the main Hall Thrusters performance range compared to Ions Thrusters, but more accurate values will be calculated in the next chapter.

### Electrostatic Thrusters: Characteristics and Performance

Type	Hall	Ion	FEEP
propellant	Xe	Xe	Cs Ir
$I_{sp}$ , s	1500-2500	2000-4000	6000
$P_E$ , W	300-10000	200-5000	1
$\eta$	0.5	0.65	0.8
voltage, V	200-600	1000-2000	6000
thruster mass, kg/kW	2-3	3-6	?
PPU mass, kg/kW	6-10	6-10	?
feed system	regulated	regulated	no
lifetime, h	> 7000	> 10000	?
missions	SK, orbit transfer (med- $\Delta V$ )	SK, orbit transfer (large- $\Delta V$ )	precise corrections

Table 6: Ion thruster vs Hall thruster performance

Finally, Hall thrusters are divided into two categories according to the material with which the chamber walls are made: there are dielectric Hall Thrusters, in which the walls are made of dielectric material, and TAL (Thrusters with Anode Layer) in which the walls are metallic. Both types of thrusters operate according to the principles described in the previous chapters, but they have major differences in three aspects: chamber geometry, main power loss and erosion mechanisms. In fact, TAL has a much smaller chamber length to diameter ratio than dielectric walls, to facilitate the electrons flow to the anode without them scattering along the walls. For the same reason, typically the walls are at almost the same potential as the cathode, so as to prevent the bombardment of electrons onto them. There are also often metallic guard rings at the chamber exit, designed to absorb sputtering and degrade instead of the chamber walls. The guard rings are also at cathode potential, in order to avoid electron loss. Following this reasoning, it is also possible to guess the differences between the power loss mechanisms: in thrusters with dielectric walls, the main mechanism is the bombardment of electrons and ions that impact against the walls, also generating erosion. In TAL, on the other hand, the main power loss occurs at the anode, and is related to the collection of discharge electrons that arrive with high energy, as well as a fraction of the ions generated near the exit that are attracted to the guard rings and deteriorate them. Finally, regarding erosion mechanisms, these are much more pronounced in TAL due to the high interaction between charged particles and metallic walls. The next picture shows the typical structure of a metallic wall's thrusters: it is possible to notice the short chamber with respect to the diameter and the presence of guard rings.

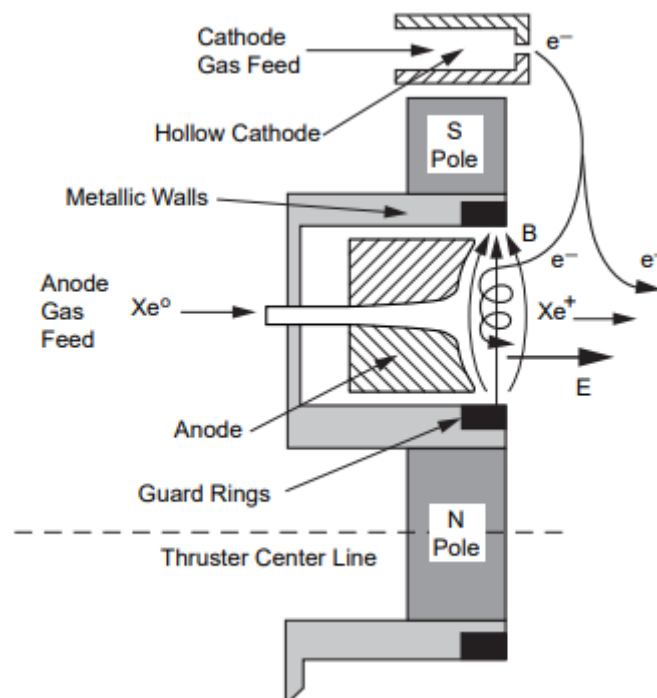


Figure 19: Sketch of a TAL

### 1.5.1 Magnetic field generator

Magnetic field generator is essential for a good working of the thruster, since many efficiencies are strictly related to electron mobility, plasma discharge current and axial distribution of plasma properties (especially density and potential). It is usually created by a coil's battery, coaxial with respect to the channel, in order to produce the desired shape and intensity at each point of the channel thanks to a different current flowing into each coil. In particular, the magnetic field must be the highest near the channel exit and right outside the channel: this configuration allows for the best plasma configuration, with the most energetic ions created near the channel exit and ready to be accelerated to create thrust. On the other hand, the magnetic field is very low near the anode: in this region it is not necessary to have all that many collisions, but it is sufficient to have just some collisions to create plasma and let the thruster work.

The graphics below show the typical magnetic field geometry inside the channel, taken from a NASA study on their NASA-173Mv Hall Thruster, together with plasma current-voltage curve for different values of **B**.

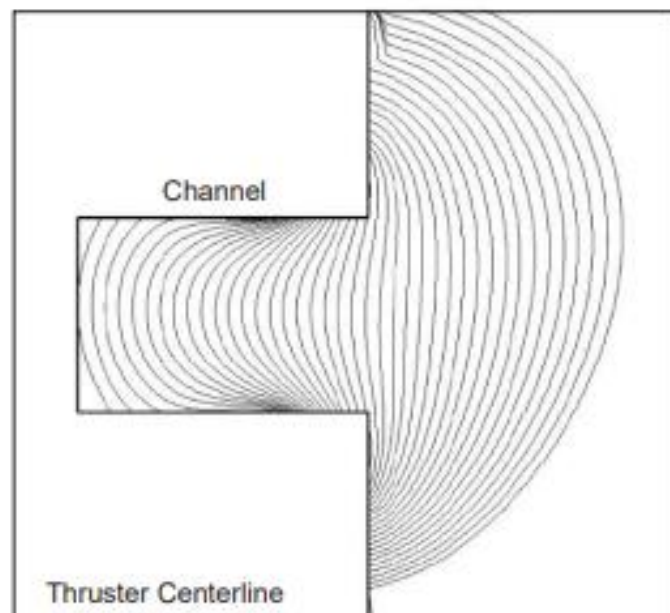


Figure 20: Magnetic field shape in NASA-173Mv

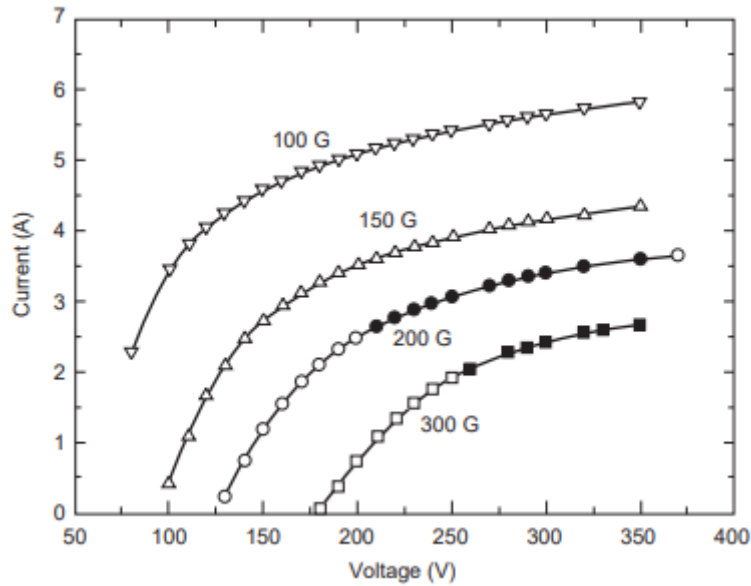


Figure 21:  $I$  vs  $V$  for different values of  $B$

According to the previous considerations, for a fixed discharge voltage, discharge current decreases as the magnetic field increases due to the lower electron mobility. This allows to minimize power losses due to electrons that reach the anode without an ionizing collision with the propellant.

### 1.5.2 Ionization

Ionization phase takes place into the plasma generator, in particular in the middle zone of the channel length. As will be shown later, in this region electrons have their maximum temperature due to the almost maximum magnetic field that minimizes their mobility inside the plasma, therefore their speed and energy will be at their maximum as well. This configuration is crucial to maximize the collision rate between electrons and propellant atoms, ensuring a sufficient electron energy to ionize the propellant during collision.

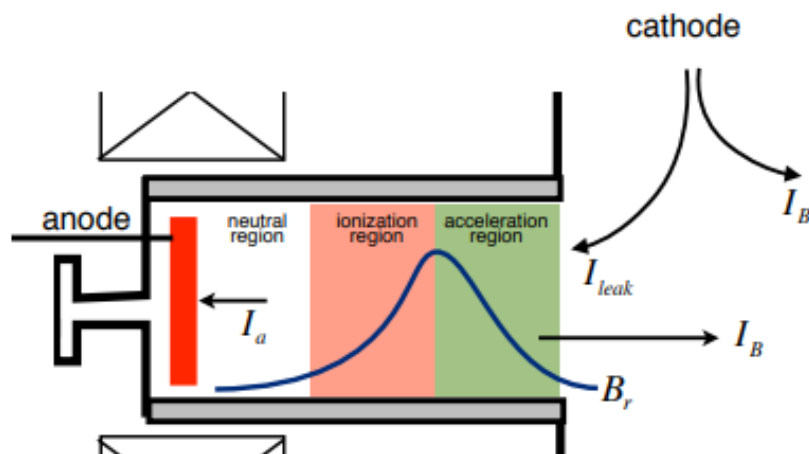


Figure 22: Channel regions along the axis

In the picture above, it is shown the axial position of each region, together with the typical trend of **B** along the axis. It must be mentioned that neutral region is the less important, since all the thrust-creation phenomena occurs in the other two regions, and it will only be described in the ‘Plasma generator’ section. The graphic below, useful for the further sections as well, represents the neutral density (volumetric density of unionized propellant) and the ionization rate (*S*) along the channel axis: neutral density has its maximum decrease right where ionization rate has its peak, while in the neutral region close to the anode neutral density is maximum and ionization rate is almost zero as mentioned.

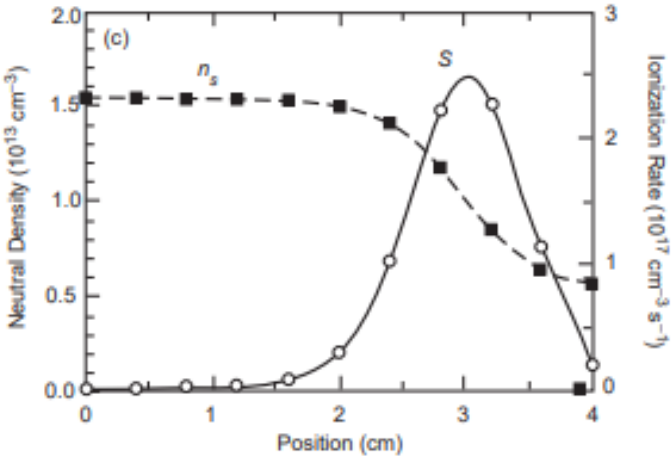


Figure 23: Neutral density and ionization rate along channel axis

### 1.5.3 Acceleration

After ions are created in the ionization zone, they fall into acceleration zone. This region is characterized by the maximum values of both **E**, **B** and potential drop. In fact, near the channel exit, plasma creates a sheath region in which ions local density is higher than electron local density. The reason behind this phenomenon is the very different ions velocity with respect to electron velocity (typically electron velocity is at least three times higher than ion velocity), which leads to a greater electrons current leaving the plasma than ions current leaving the plasma. This creates a local ions accumulation, which accelerates other ions falling into that region toward the exit. In the next graphic, it is shown the trend of electric field and potential drop along the axis: as mentioned, potential drop has its maximum rate toward the exit, while electric field has its peak right before the exit.

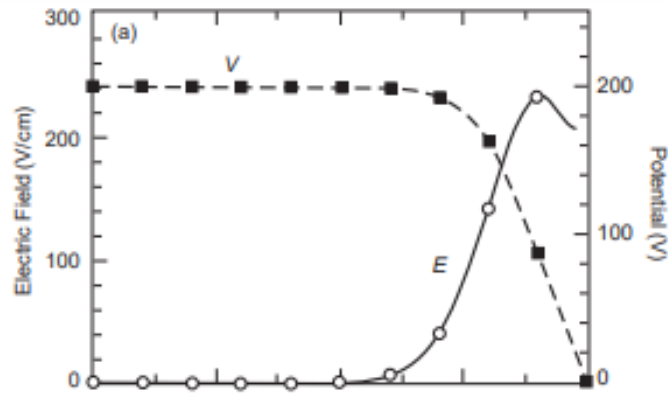


Figure 24: Electric field and voltage drop along the channel axis

To complete the information, it is also shown what happens right outside the channel region: as one can imagine,  $\mathbf{E}$  and  $\mathbf{B}$  quickly drop to zero. In fact, vacuum makes the beam diverge and charge density reaches its minimum (close to 0), hence the  $\mathbf{E}$  drop, while  $\mathbf{B}$  drop is justified by the fact that outside of the channel there is no magnet or current creating a radial  $\mathbf{B}$ .

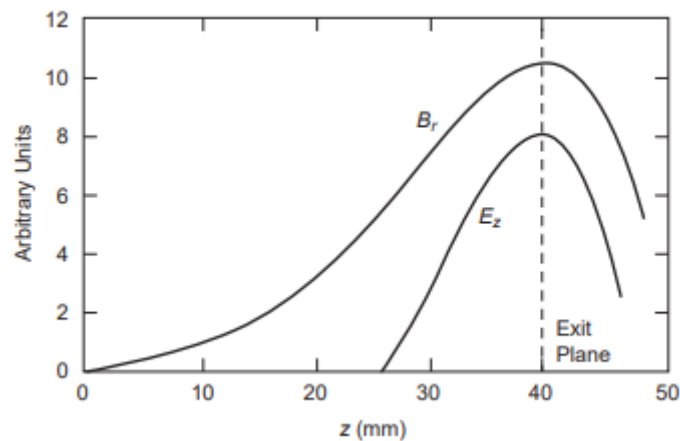


Figure 25: Radial  $B$  and axial  $E$  along channel axis

### 1.5.4 Neutralization

Neutralization is essential in electrostatic propulsion, in order to avoid spacecraft charging due to ion emission. In Hall Thrusters, neutralization is provided by the main cathode: in fact, only a fraction of the emitted electrons flows into the discharge chamber, while the remaining part goes into the exit ion beam. Not only this ensures spacecraft neutrality, but also beam electrons nullify the potential created by the emitted ions. This allows to overcome Child-Langmuir law, since space-charge limitations do not occur, so emitted current is hypothetically unlimited. In practical terms, the best advantage of this configuration over Ions Thrusters is that it is not necessary a secondary cathode to ensure neutralization, and this reduces technical and construction issues a lot.

In the picture below, it is possible to see the typical electron's trajectory from the emitting cathode toward both the anode and the beam.

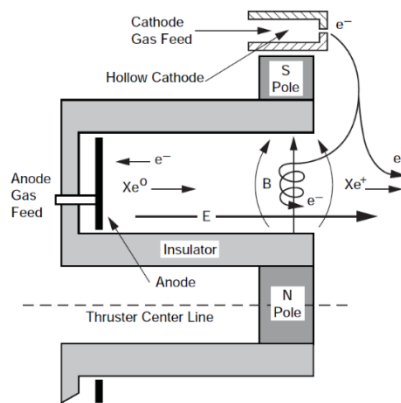


Figure 26: Electrons' typical trajectory

### 1.5.5 Hollow cathode

Cathode is one of the most important components in Hall Thrusters, not only for its emitting function, but also for its durability. In fact, its erosion and degradation are the main limit to thruster life extension, thus it must be designed in the best possible way. The other important aspect is related to efficiency: cathode power results in a complete loss of power, since it does not generate thrust, so it is important to reduce it as much as possible in order to improve the overall efficiency of the thruster.

In the first Hall Thrusters, the emitting cathode was made up of tungsten filaments, which begin to emit electrons when their temperature is over about 2600 K. Also, small fractions of filament were injected into the beam as well, to provide neutralization. The problems with this system are several:

- Cathode life: the cathode life is strictly limited by tungsten evaporation and sputtering erosion, due to the extremely high temperature. Typically, the life of this type of cathode is about hundreds of hours or even less, making it impossible to use it for long missions;
- Power consumption: due to the tungsten high work function, the power required to keep the cathode emitting an electron current is comparable to the discharge power (power required to maintain the plasma current in the chamber region), so global efficiency is penalized;
- Thermal control: the high temperatures reached require a huge thermal shield to limit radiation power losses.

Nowadays, hollow cathode is the most popular solution to overcome tungsten cathodes limits. It has a cylindrical shape with an orifice placed at its end and a cylindrical insert is pushed inside the cathode toward the end. A heater is also essential to raise insert temperature and make it emit electrons (thermionic emission). The final cathode component is the external keeper, which serves to prevent cathode erosion. However, this will be discussed in greater detail at a later point in the text. The cathode functions by creating plasma. A small quantity of propellant is introduced into the



cathode, which provides ionisation to generate plasma due to the heated and emitting insert surface, which is in turn heated by the heater. The insert surface is made of special materials that have a low work function (Barium oxide BaO or Lanthanum hexaboride LaB<sub>6</sub>) in order to minimize the required power to emit high electron currents (typical values are tens of A/cm<sup>2</sup>, whereas tungsten filaments cathode could roughly provide 1 A/cm<sup>2</sup> or even less). Plasma cathode is characterized by high density and low voltage: the low voltage prevents the ions from bombarding the inner surface with too much energy, which would limit cathode life, while high density eliminates space-charge limits allowing theoretical unlimited electron emissions. The following image shows the typical hollow cathode geometry, with emissive insert and wrapped heater.

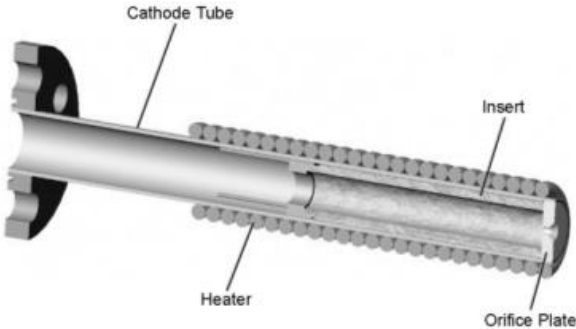


Figure 27: Hollow cathode geometry

Cathode plasma can be divided into three main zones: dense zone, high current zone and plume zone. The first one takes place along almost all the cathode length, since the small orifice diameter (1 ÷ 3 mm) reduces plasma spillage from the cathode. The second one is located in the last millimeters of the tube, where the insert emits electrons creating an extremely high current in the plasma. This region is considered to be the most critical for cathode erosion, together with the outer surface. The last region is basically the plume outside of the cathode, through which electrons flow toward the anode and the external beam. These three regions are shown in the picture below.

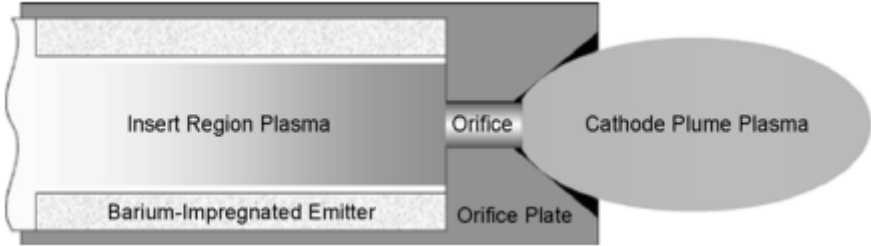


Figure 28: Hollow cathode regions

Finally, outside of the cathode, there is a keeper. It is usually at a positive potential relative to the cathode and it has a threefold role: to facilitate the initiation of the

discharge in the cathode, to act as a heat shield to limit radiation, and finally to protect the cathode from the bombardment of ions from the chamber. The latter mechanism is the most dangerous for the life of the cathode, since the ions would come against its surface with an energy of hundreds of eV, giving rise to major erosion phenomena. A typical configuration for the cathode keeper is shown in the following image.

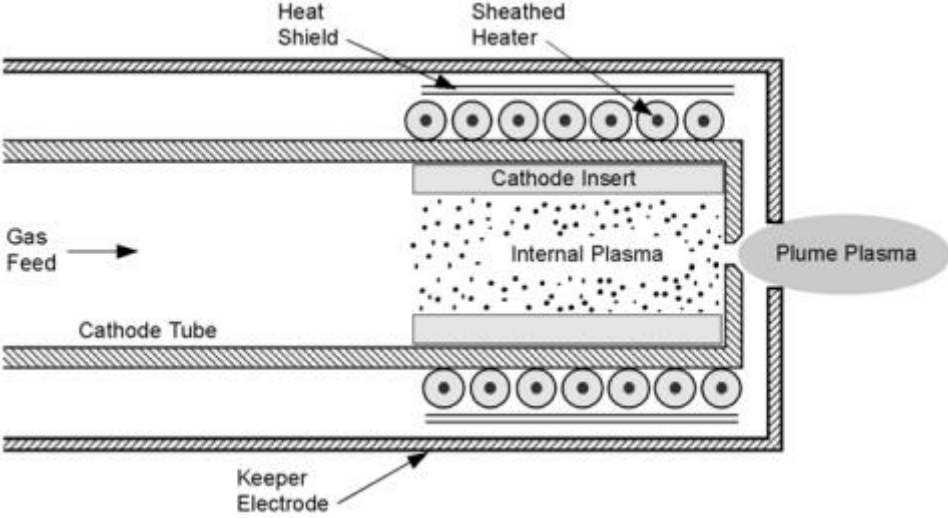


Figure 29: Cathode with keeper electrode

At last, in the picture below it is possible to see the three main cathode configurations, which differ from each other for the orifice diameter to length ratio. For simplicity, the three configurations will be called small, medium and large orifice.

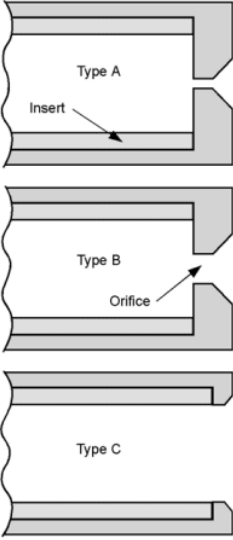


Figure 30: Different cathode shapes

As mentioned earlier, the cathode needs to maintain a high temperature to function properly. Typically, cathodes used today operate at temperatures of about 1500-1800 °C, but a heating mechanism is required to sustain electron emission. The three possible methods are orifice heating, ion heating and electron heating. Orifice heating

is characterized by the deposition of energy near the exit orifice thanks to the Joule effect. This mechanism typically occurs in cathodes with small orifice, because plasma density inside them is very high and therefore its resistance will also be high enough to trigger overheating of the plasma by Joule effect. The heat is then transferred to the walls by convection. Ion heating is the most common mechanism and it is based on ion drop across the sheath potential. Plasma ions are in fact attracted to the cathode, which is at a lower potential than that of the plasma: therefore, ions that manage to overcome the outer sheath of the plasma impact against the inner surface of the cathode, depositing energy on it via their bombardment. The most critical aspect related to this mechanism is again the erosion of the cathode by the ions. Lastly, electron heating is the least common mechanism and it is typical of high flow rate cathodes. In this condition the plasma pressure is quite high, as it is the current within it, and the sheath potential is relatively low. Electrons that are in the energetic tail of the Maxwellian distribution are then able to escape from the plasma, impacting against the inner surface of the cathode. In this way, their energy is transferred to the cathode in the form of heat.

Thermionic electron emission by the insert is strictly dependent on its shape, temperature and material. The emitted density current can be computed using Richardson-Dushman equation:

$$J = A \cdot T^2 \cdot e^{-\frac{e \cdot \Phi}{k \cdot T}}$$

where  $J$  is the emitted density current,  $T$  is the surface temperature,  $\Phi$  is the work function of the insert material,  $A$  is a constant dependent on many factors (temperature, material shape, insert chemical composition) and its ideal value is  $120 \frac{A}{cm^2 K^2}$ . Since the value of  $A$  can significantly change, a semiempirical correction is necessary to fit expected results with data measurements, so it is:

$$\Phi = \Phi_0 + \alpha \cdot T$$

where  $\Phi_0$  is the tabled value of the work function, while  $\alpha$  is computed experimentally. The original equation then becomes:

$$J = D \cdot T^2 \cdot e^{-\frac{e \cdot \Phi_0}{k \cdot T}}$$

In the table below are reported the  $A$  and  $D$  values for the most used materials, while the next graphic shows the emission density current trend versus temperature for different types of cathodes.

	$A$	$D$	$\phi$
BaO-Scandate [11]	120	—	$8 \times 10^{-7} T^2 - 1.3 \times 10^3 T + 1.96$
BaO-W 411 [12]	120	—	$1.67 + 2.82 \times 10^{-4} T$
BaO-W 411 [10]	—	1.5	1.56
LaB <sub>6</sub> [13]	—	29	2.66
LaB <sub>6</sub> [14]	—	110	2.87
LaB <sub>6</sub> [15]	120	—	2.91
LaB <sub>6</sub> [8]	120	—	$2.66 + 1.23 \times 10^{-4} T$
Molybdenum [8]	—	55	4.2
Tantalum [8]	—	37	4.1
Tungsten [8]	—	70	4.55

Table 7: Fitting coefficients for electrons emission

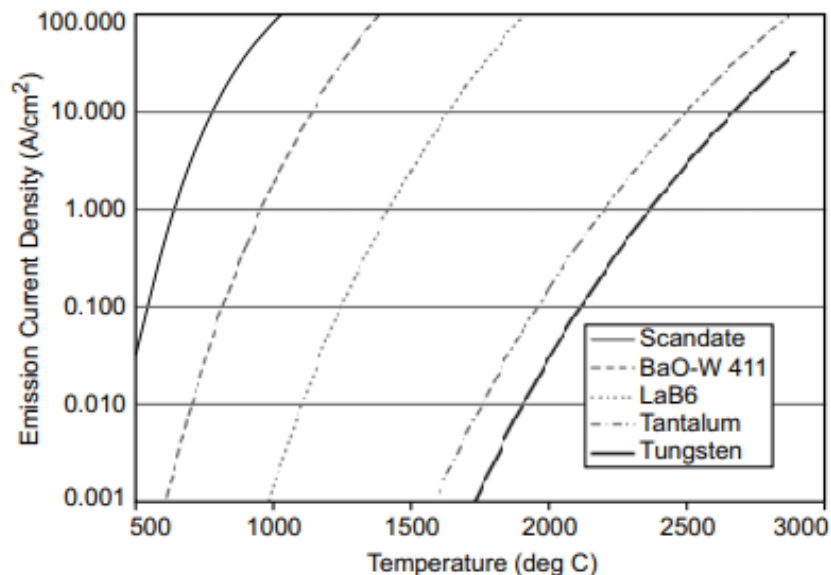


Figure 31: Emission current density vs  $T$  for different materials

At last, a full comparison of the two most used materials must be made.

### BaO insert cathode

The cathode with BaO insert is constructed by coating the inner surface of the insert with this substance, which can withstand high temperatures and lowers the work function that characterizes electron emission. However, BaO has a high evaporation rate, which makes it essential to use a dispenser to avoid consuming the entire surface film. The BaO is accumulated in the dispenser, while the insert is made of a porous material in contact with the dispenser. It can be demonstrated that the BaO film is continuously regenerated as it passes from the dispenser through the pores of the insert. The two major advantages of this solution lie in cost and the relative ease of cathode construction, which is why early hollow cathodes often used this configuration. However, the dispenser cathode has significant disadvantages. The first is that it

cannot withstand too high temperatures, because the high evaporation rate of BaO would lead to the consumption of the entire dispenser before the mission is completed. In addition, BaO is extremely sensitive to impurities in the feeding gas: the main poisons are  $H_2O$  and  $O_2$  and they result in complete poisoning for partial pressures of  $10^{-7}$  torr or more. Therefore, to ensure a good cathode functioning and reduce its degradation rate, it is necessary to use a 'propulsion-grade' xenon, which has a purity level of at least 99,9995%. Even if it is easily manageable, the last downside is that this type of cathode requires a starting procedure, consisting of a specific timing of temperature and voltage raising and propellant emission, otherwise plasma is not properly created and too much power gets lost.

### **LaB<sub>6</sub> cathode**

LaB<sub>6</sub> cathode is the most widely used in recent thrusters because it provides better performance. Its geometry and functioning are the similar to BaO cathode ones, with the difference that this cathode does not need a dispenser due to the low evaporation rate of LaB<sub>6</sub> deposited on its surface. The first major advantage lies in the fact that there are no chemicals that reduce the work function of the insert, since it itself has a low working function and can emit electrons. This aspect allows much larger impurities to be tolerated in the propellant, amounting to about 100 times the tolerable impurities in BaO cathodes, but it also requires a higher temperature to achieve the same level of electron emission. Second, LaB<sub>6</sub> has a much lower evaporation rate than BaO, allowing a cathode life of about 10 times that of dispenser cathodes. The last positive aspect lies in the fact that these cathodes do not require an ignition procedure: it is sufficient to inject the propellant inside them and start the heater to have the necessary electron emission for the creation of the plasma. The main disadvantage of this type of cathode lies in the construction difficulty. In fact, LaB<sub>6</sub> is a crystalline material that is obtained by sintering LaB<sub>6</sub> powder into bars or plates and then processing the material into the desired shape. This makes processing very expensive and complicated, although current technologies allow for easy production of these cathodes. Finally, what makes the implementation of these cathodes complicated is the need to have an electrical contact with materials that inhibit boron diffusion, even at high temperatures.

### **Erosion process**

As mentioned, erosion is one of the most critical aspects in thruster life, and it affects both the main channel and cathode channel. Its modeling is essential to understand walls' shape changes while erosion occurs and many models, both theoretical and empirical, can be found in literature. The one presented here is the Gamero model, which computes erosion rate in a semi-empirical way, considering ion energy and incident angle of ions towards the walls as parameters. The erosion rate  $\dot{R}$  is defined as the change in wall thickness  $w$  over time:

$$\dot{R} = - \frac{\partial w}{\partial t}$$

and, in this model, is computed as:

$$\dot{R} = \frac{J_i \cdot W}{\rho \cdot e \cdot A_v} \cdot y(\epsilon_i)$$

where  $J_i$  is current density in the plasma,  $W$  is the propellant atomic weight,  $\rho$  is plasma mass density,  $A_v$  is Avogadro constant ( $6,022 \cdot 10^{23}$ ) and  $y(\epsilon_i)$  is the sputtering yield.  $y(\epsilon_i)$  depends on ion energy and impact angle as follows:

$$y = (0,0099 + 6,04 \cdot 10^{-6} \cdot \alpha^2 - 4,75 \cdot 10^{-8} \cdot \alpha^3) \cdot \sqrt{\epsilon_i} \cdot \left(1 - \sqrt{\frac{58,6}{\epsilon_i}}\right)^{2,5}$$

being  $\alpha$  the incident angle of ions towards the wall and  $\epsilon_i$  the ion energy that impacts the wall. For both these parameters, a mean value can be used to simplify the operations. The following images show the erosion of the cathode channel and keeper after a 30.000 working hours test. For what concerns the cathode channel, it is clear that a good design is mandatory to ensure its functioning over the total mission time, even after important erosion phenomena occurs. On the other hand, it is possible to see how the keeper is completely destroyed after thruster life ends, pointing out its importance to avoid cathode from the same destruction process and to let it work properly.

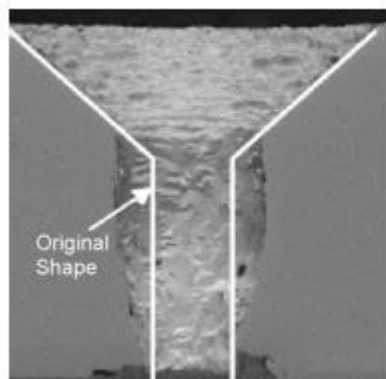


Figure 32: Cathode channel erosion @30.000 hours

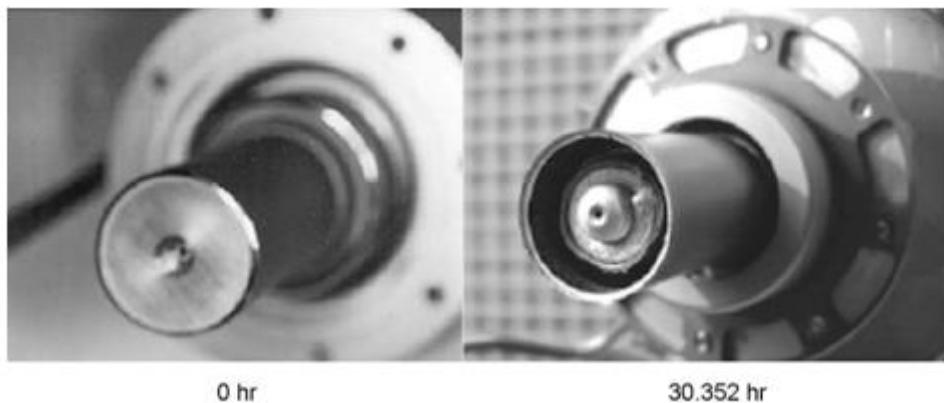


Figure 33: Cathode keeper erosion

## **2. Mathematic model**

### **2.1 Introduction and assumptions**

This chapter will present the model employed to examine the performance and efficiency of Hall Thrusters. As mentioned, this is a simplified model, which takes into account only the main phenomena involved in HT functioning, therefore results will be a bit more optimistic than real ones. In particular, the discharge chamber is modeled with a 1-D model to justify the presence of the three main regions described above (neutral or sheath, ionization and acceleration region). The focus in this phase will be on plasma properties and behaviour. Later on, there will be an analysis of the main power loss mechanisms, so as to understand which phenomena and parameters are the most important to be improved in order to have a better efficiency. At last, some new efficiency definitions will be presented: these ones are more specific than the previous mentioned, and they are much more useful to describe Hall Thrusters performance in detail, since they are referred to very specific functioning aspects. It is important to mention that many relations, especially for what concerns power loss mechanisms, are semiempirical, since some aspects of these phenomena are still unknown. However, the presented relations fit extremely well the test measured data, so they provide good results within the considered functioning range.

## 2.2 Plasma generator

Plasma generator (also called 'chamber') is the core of Hall Thrusters functioning, and it is extremely important to understand plasma behaviour in this region in order to have a precise computation of the power loss.

First of all, plasma occurs in a vacuum chamber, thus it respects Maxwell equations:

- $\nabla \cdot \mathbf{E} = \frac{\rho}{\epsilon_0}$
- $\nabla \cdot \mathbf{B} = 0$
- $\nabla \times \mathbf{E} = -\frac{\partial \mathbf{B}}{\partial t}$
- $\nabla \times \mathbf{B} = \mu_0(\mathbf{J} + \epsilon_0 \frac{\partial \mathbf{E}}{\partial t})$

Once a charged particle enters a magnetic field zone, its motion can be described considering Lorentz force as follows:

$$\mathbf{F} = m \frac{d\mathbf{v}}{dt} = q(\mathbf{E} + \mathbf{v} \times \mathbf{B})$$

which describes, in the case of a negligible electric field, the simple harmonic oscillator. Its frequency, called cyclotron frequency, is:

$$\omega_c = \frac{qB}{m}$$

As known, the charged particle will move in a circular trajectory if its speed is perpendicular to the magnetic field, or helicoidal trajectory if it has a component on  $\mathbf{B}$  direction as well. Trajectory radius is also known as Larmor radius ( $r_L$ ) and can be derived applying Newton's second law, leading to:

$$r_L = \frac{m \cdot v_{\perp}}{q \cdot B}$$

while helix pitch  $P$  is derived from the study of particle circular motion and will be:

$$P = \frac{2\pi m v_{\parallel}}{qB}$$

being  $v_{\perp}$  and  $v_{\parallel}$  respectively perpendicular and parallel to  $\mathbf{B}$  component of particle velocity. Once an electric field  $\mathbf{E}$ , perpendicular to  $\mathbf{B}$ , is considered, then particle velocity will also have a drift component, perpendicular to both  $\mathbf{E}$  and  $\mathbf{B}$  and computed as:

$$v_d = \frac{\mathbf{E} \times \mathbf{B}}{B^2}$$

This velocity component leads to the typical stretched trajectory shown in figure, where it is possible to notice the difference between ion and electron trajectory's radius due to their very different mass. This difference will be described by the Hall parameter, and it explains why the magnetic field affects the electron motion in the chamber but leaves ions almost undisturbed.



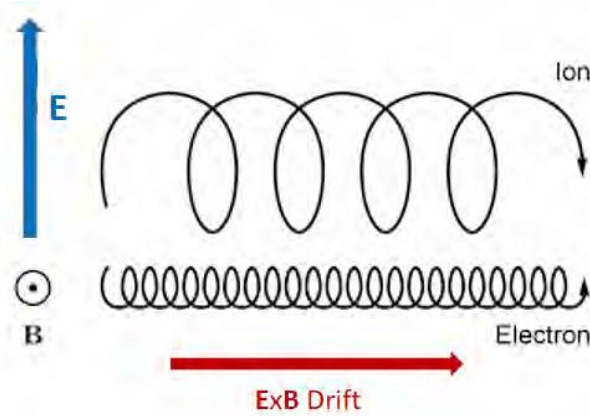


Figure 34: Electrons and ions trajectory in an electro-magnetic field

As one can imagine, plasma particles undergo a large number of collisions, making it impossible to track their single motion. It is more convenient to have a global vision, based on mean values and distribution of the considered parameters. The typical distribution is Maxwellian distribution, which is the most probable for a group of particles in thermal equilibrium. Maxwellian distribution for velocity in 1-D is:

$$f(v) = \left(\frac{m}{2\pi kT}\right)^{\frac{1}{2}} \cdot e^{\left(-\frac{mv^2}{2kT}\right)}$$

being  $m$  the particle mass,  $T$  the temperature in K and  $k$  Boltzmann's constant (Boltzmann's constant:  $k = 1,38 \cdot 10^{-23} J/K$ ). This distribution leads to a mean energy value of:

$$E_{av} = \frac{1}{2} kT$$

for each direction. Typically, in HT plasmas, electrons' temperature will be about ten times ions' temperature, due to the high energy level they are provided to ionize propellant. The assumption made by now on is that plasma is quasi-neutral: it means that ion density  $n_i$  is almost equal to electron density  $n_e$ . This is a strong simplification, because the extremely different velocity of the two species creates an imbalance toward higher ions density, which is only partially compensated by electric field forces. Once an electric field (thus a potential) is applied to a plasma, electron density will change in order to preserve electron partial pressure in the plasma, as described by the barometric law:

$$n_e = n_e(0) \cdot e^{\left(\frac{q \cdot \Phi}{k \cdot T_e}\right)}$$

where  $T_e$  is the electron temperature and  $\Phi$  is the applied potential relative to the initial density  $n_e(0)$ . This equation is useful to explain what happens at plasma boundaries: due to potential gradients and high electron velocity, a zone with low electron density occurs. This is called sheath zone and, due to its positive potential, it attracts back electrons, maintaining quasi-neutrality of the plasma. The typical sheath configuration is shown in the picture below.

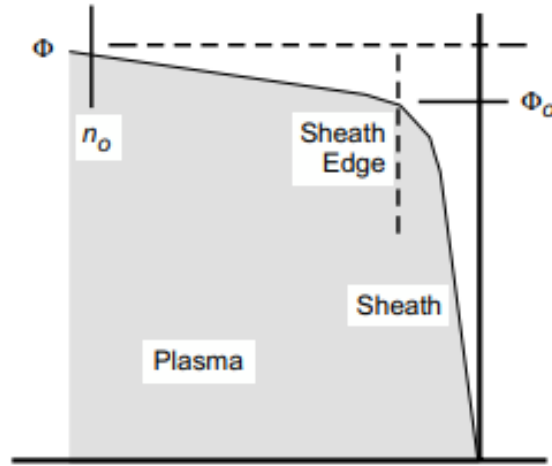


Figure 35: Plasma sheath potential

As already mentioned, collisions are crucial in Hall thrusters functioning, since they are responsible for ions creation. It is important to have a clear overview on this mechanism in order to estimate power losses in the plasma. Two main cases must be studied: a slow particle moving in a quasi-neutral plasma and a fast particle moving in a quasi-neutral plasma. In both cases, if a collision occurs, it can be elastic or inelastic relatively to energy conservation, and ionizing or exciting relatively to its effect on colliding particles. Considering a thin portion of the plasma, characterized by a section  $A$  and a thickness  $dx$ , the number of atoms contained in that portion will be  $N = n_a \cdot A \cdot dx$ , and each atom will cover a cross-sectional area  $\sigma$ . The covered area will then be  $n_a \cdot \sigma \cdot dx$  and, if a particle flux  $\Gamma_0$  flows through this portion, the flux that emerges without having a collision will be:

$$\Gamma(x) = \Gamma_0(1 - n_a \cdot \sigma \cdot dx)$$

and its change will be:

$$\frac{d\Gamma}{dx} = -\Gamma \cdot n_a \cdot \sigma$$

The solution to this simple equation is:

$$\Gamma = \Gamma_0 \cdot e\left(\frac{-x}{\lambda}\right)$$

where  $\lambda = \frac{1}{n_a \cdot \sigma}$  is the mean free path for collisions and it represents the mean distance that a fast-moving particle will travel in a stationary density of neutral particles before having a collision. The time before particle collision will then be:

$$\tau = \frac{1}{n_a \cdot \sigma \cdot v}$$

and, if a mean velocity is considered, collision frequency will be:

$$f = n_a \cdot \sigma \cdot v$$

If a slow particle (such as neutral propellant atoms) is considered, the previous equations will have the same structure, but different parameters. In this case, the mean free path is computed as  $\lambda = \frac{v_n}{n_e \langle \sigma v_e \rangle}$ , where  $v_n$  is the neutral particle velocity and the reaction rate coefficient in the denominator is averaged over all the relevant collision cross sections. The last difference to point out regards the type of collision. In fact, especially for low electron's energy, the collision between electron and neutral atom could occur at a high divergence angle between their velocities. This type of collision does not ionize the atom, but it just excites it, increasing its velocity. The volumetric ion production rate can be calculated as:

$$\frac{dn_i}{dt} = n_a n_e \langle \sigma_i v_e \rangle$$

where  $\sigma_i$  is the ionization cross section and the term in brackets represents the reaction rate coefficient, which is the average ionization cross section for the given velocity distribution. Charge exchange collisions are the dominant factor in heating of cathode. In a similar manner, a volumetric excited neutrals production rate can be computed as:

$$\frac{dn_*}{dt} = n_a n_e \langle \sigma_* v_e \rangle$$

where  $\sigma_*$  is the excitation cross section,  $n_*$  is the excited neutral atoms density and the term in brackets represents the reaction rate coefficient in the case of exciting collisions. If a Maxwellian velocity distribution is considered for electrons, these reaction rates can be calculated with semi-empirical formulas as follows:

$$\langle \sigma_i v_e \rangle \text{ for } T_e < 5 \text{ eV: } \langle \sigma_i v_e \rangle = 10^{-20} \left[ (3,97 + 0,643 T_{eV} - 0,0368 T_{eV}^2) \cdot e^{-\frac{12,13}{T_{eV}}} \right] \cdot \left( \frac{8eT_{eV}}{\pi m} \right)^{\frac{1}{2}}$$

$$\langle \sigma_i v_e \rangle \text{ for } T_e > 5 \text{ eV: } \langle \sigma_i v_e \rangle = 10^{-20} \left[ (-1,031 \cdot 10^{-4} \cdot T_{eV}^2) + 6,386 \cdot e^{-\frac{12,13}{T_{eV}}} \right] \cdot \left( \frac{8eT_{eV}}{\pi m} \right)^{\frac{1}{2}}$$

$$\langle \sigma_* v_e \rangle = 1,93 \cdot 10^{-19} \cdot \frac{e^{-\frac{11,6}{T_{eV}}}}{\sqrt{T_{eV}}} \cdot \left( \frac{8eT_{eV}}{\pi m} \right)^{\frac{1}{2}}$$

At this point, some collision frequencies can be calculated. Being  $\nu_{en}$ ,  $\nu_{ei}$ ,  $\nu_{ee}$ ,  $\nu_{ii}$  respectively the collision frequencies between electron-neutrals, electron-ions, electron-electron and ion-ion, their value are helpful to understand the equilibration time among species and between different species.

They can be calculated as follows:

$$v_{en} = \sigma_{en}(T_e) \cdot n_e \cdot \sqrt{\frac{8kT_e}{\pi m}}$$

where  $\sigma_{en}(T_e) = 6,6 \cdot 10^{-19} \left[ \frac{0,25T_{eV}-1}{1+(0,25T_{eV})^{1,6}} \right]$ ;

$$v_{ei} = 2,9 \cdot 10^{-12} \frac{n_e \cdot \ln(Y)}{T_{eV}^{\frac{3}{2}}}$$

where  $\ln(Y) = 23 - 0,5 \cdot \ln\left(\frac{10^{-6}n_e}{T_{eV}^3}\right)$ ;

$$v_{ee} = 5 \cdot 10^{-12} \frac{n_e \cdot \ln(Y)}{T_{eV}^{\frac{3}{2}}}$$

$$v_{ii} = Z^4 \left(\frac{m}{M}\right)^{0,5} \left(\frac{T_e}{T_i}\right)^{0,5} \cdot v_{ee}$$

where  $Z$  is the ion charge number and  $\frac{m}{M}$  is electron-ion mass ratio.

Finally, the reciprocals of these values represent slowing time  $\tau_s$ , which is the time for a monoenergetic electron to equilibrate with the Maxwellian electrons population present in the plasma, and equilibration time  $\tau_{eq}$ , which represents the time for one Maxwellian population to equilibrate with another. The difference between these frequencies, due to the extremely different mass between ions and electrons, explains why electrons thermalize quickly into a Maxwellian population, but don't thermalize as quickly with ion Maxwellian population, allowing a huge temperature ratio between the two species as was mentioned before.

Once collision rates are determined, it is possible to calculate the Hall parameter for the different species. This parameter is a measure of how much the magnetic field affects particle motion, considering the collisions rate that has a direct impact on particle velocity. The Hall parameter  $\Omega$  is defined as follows:

$$\Omega = \frac{\omega_c}{v_c} = \frac{qB}{mv_c}$$

being  $v_c$  the sum of collisions rates for the studied particle and  $m$  the particle mass. It is possible to notice that, for the electrons, this parameter is much bigger than 1 due to their low mass and low collision rate. This means that their velocity will be high and the magnetic field strongly interacts with them, changing their trajectories as shown. On the other hand, for the ions, this parameter is much lower than one, due to their high mass and collision rate. Since many collisions occur, their velocity will drop to

almost zero quite often and the magnetic field does not change their trajectory all that much.

The last plasma parameter useful to describe its behaviour is Debye length, which is the distance over which plasma potential changes when a small potential change (small with respect to electron temperature in eV) occurs at its borders. In fact, once a potential change is applied to the plasma at its boundary (or even inside the plasma, if a charged particle is pushed inside it), it locally changes its charge density: for example, if a positive potential is applied, there will be an electron accumulation. This mechanism creates a sort of 'shield', and after electrons become locally denser, the rest of the plasma won't experience the applied potential. Debye length  $\lambda_D$  is defined as follows:

$$\lambda_D = \sqrt{\frac{\epsilon_0 \cdot k \cdot T_e}{n_0 e^2}}$$

All that has been described in this section is useful to explain the three regions chamber model. Near the anode, the magnetic field is low and electrons are free to flow toward the anode. In this region, plasma density is low as well, since electrons are not energetic nor dense and only few ionization collisions occur. Also, it wouldn't be convenient to have a huge ions production in this region, because their path toward the exit would be relatively long, leading to high power losses due to collisions and local potential changes, and also a higher erosion rate due to the higher number of ions that impact the channel surface. In the middle of channel length, the magnetic field approaches its maximum and energetic electrons are accumulated due to their low mobility through it. As seen, a high electron density, together with high electron temperature, leads to a high ionization collision frequency, so the majority of the ions are created in this region. At last, in the acceleration region near the channel exit, ions experience a huge potential drop due to anode electric field and plasma sheath potential, so they will be strongly accelerated toward the outer space producing thrust.

## 2.3 Power losses

Once the operations of the Hall thrusters have been described, it is possible to evaluate the total power loss by studying the main power loss mechanisms. Four different mechanisms are considered here: power loss to channel wall, power loss to anode, radiated plasma power and ionization power. Other types of power loss, such as electron power into the beam and ion power towards the anode, are not considered because they are almost two orders of magnitude smaller than those mentioned above. After presenting each formula, the relative loss is calculated using typical values from existing Hall thrusters to provide a measure of the importance of this power loss mechanism.

## Power to channel wall

This type of loss represents the power lost due to electrons and ions bombarding the wall. It is the most significant in dielectric walls Hall Thrusters, since the walls can't absorb any charge. This means that, if a charged particle hits the wall, it will be repelled and, during the collision, it will deposit an amount of its energy to the wall. This power can be computed as follows:

$$P_w = n_e e A \left[ \frac{kT_e}{e} \left( \frac{kT_e}{2\pi m} \right)^{\frac{1}{2}} e^{\frac{e\Phi_s}{kT_e}} + \frac{v_i}{2} (\varepsilon - \Phi_s) \right]$$

where the first term in brackets represents the energy deposited by the electrons that overcome the repelling sheath potential, while the second term represents the energy of the ions due to their fall through the sheath potential.  $\varepsilon$  is the ion energy when it is at the end of pre-sheath and  $\Phi_s$  is the sheath potential with respect to the plasma potential. Considering SPT-100, in which plasma is created by Xenon and  $\text{BNSiO}_2$ , this equation can be adapted as follows:

$$P_w = 48,5 \cdot I_{iw} T_{eV}$$

being  $I_{iw} \approx 0,1 \cdot I_b$  the ion current toward the wall, and  $T_{eV} \approx 0,1 \cdot V_b$  the ion temperature in eV. This leads to a power loss  $P_w = 0,49 \cdot I_b V_b$ , which almost represents the total amount of power loss. For TAL this term is negligible, because typically charged particles are absorbed by the walls, generating a different kind of power loss, and also because walls are usually at the same cathode potential, so electrons will be strongly repelled while ions tend to be accelerated toward the exit.

## Power loss to anode

This power loss is due to the discharge current towards the anode and it's the main power loss mechanism in TAL thrusters. In fact, in dielectric wall thrusters, the hot plasma zone is far from the anode, and the electrons flowing toward the anode are at a low energy level. Instead, in a TAL thruster, the channel is much shorter and the most energetic portion of the plasma is almost in direct contact with the anode. This leads to a high power deposition to the anode, which is typically at a very high temperature due to heat absorption. Power loss to anode  $P_a$  is computed as follows:

$$P_a = 2 \cdot T_{eV} \cdot I_d$$

For TAL Thrusters  $T_{eV} \approx 0,1V_b$  near the anode, and  $I_d \approx \frac{I_b}{0,7}$ , leading to an anode power loss of:

$$P_a = 0,29 \cdot I_b \cdot V_b$$

while for dielectric walls thrusters  $T_{eV} \approx 0,01V_b$  and  $I_d \approx I_b \cdot 0,7$  , so anode power loss will be:

$$P_a = 0,014 \cdot I_b \cdot V_b$$

### **Radiative plasma power**

This is the power loss due to exciting collisions that don't produce ionisation. It is usually negligible in both dielectric walls and TAL thrusters, since excitation rate is much smaller than ionization rate at  $T_{eV} \approx 30 eV$  , which is the typical electron temperature in Hall Thrusters chambers. It can be calculated as follows:

$$P_R = n_0 n_e \langle \sigma_* v_e \rangle V$$

Typical values are  $P_R \approx 0,005 \cdot I_b \cdot V_b$  .

### **Ion production power**

The last mechanism of power loss concerns the production of ions. As mentioned, this power is completely lost because ion creation does not provide thrust, and recombination in the beam is not possible. Therefore, ionization energy cannot be restored and will be lost as a frozen flow loss. The power to produce ions will be computed as:

$$P_{ion} = (I_b + I_{iw})U^+$$

where the term in brackets represents the sum of ion beam current and ion current towards the wall, while  $U^+$  is ionization potential and its typical value is  $U^+ \approx 60 V$  or 5% of beam voltage. Under these assumptions, power to produce ions will be:

$$P_{ion} \approx 0,09 \cdot I_b \cdot V_b$$

## 2.4 Efficiency for Hall Thrusters

Once the model is set up, it is important to define some efficiencies in order to evaluate the goodness of the engine. The following parameters are intended to replace the general efficiencies described in section 1.4, as they are specific to evaluate Hall thruster performance.

### Cathode efficiency

This is the ratio between propellant mass flow rate to anode and total mass flow rate. It is essential to describe the quality of the cathode and electron emittance process, since it represents the propellant fraction that is lost in the cathode. In fact, all the propellant that flows into the cathode does not provide any thrust, but it is only used to create plasma in the cathode. Based on how it is defined, this parameter should be the highest possible.

$$\eta_c = \frac{\dot{m}_a}{\dot{m}_p} = \frac{\dot{m}_a}{\dot{m}_a + \dot{m}_c}$$

Typical values are close to 0,9.

### Electrical utilization for other powers

This parameter is useful to describe how much of the input power is effectively converted into beam power and thus thrust. In fact, it is a measure of the quality of the electrical system as it takes into account the power of the cathode keeper and the power required to generate the magnetic field.

$$\eta_o = \frac{P_d}{P_d + P_{keeper} + P_{magn}}$$

It must be noticed that  $P_{keeper}$  is set to zero during operations, since keeper is used only during ignition to start the electron emission, but once the thruster is on, the cathode will heat by itself thanks to the heating methods described in section 1.5.5. This efficiency is also known as charge efficiency, and it's typically close to 1 since also  $P_{magn}$  is usually very small if compared to discharge power.



## Anode efficiency

Anode efficiency is typically used to evaluate the basic thruster performance, neglecting cathode and magnetic field generator power. This parameter highlights trends in plasma production and ion acceleration, apart from all other types of losses, so it is a measure of the goodness of the thruster. Nevertheless, it shall not be confused with total efficiency, since total efficiency takes into account all (or almost all) the power losses. Anode efficiency can be computed as follows:

$$\eta_a = \frac{T^2}{2\dot{m}_p P_d} = \frac{\eta_t}{\eta_o \eta_c}$$

## Voltage and current efficiency

These parameters basically express the fraction of discharge current that becomes beam current and the fraction of discharge voltage that is converted into axially directed ion velocity. Their expressions are:

$$\eta_b = \frac{I_b}{I_d}$$
$$\eta_v = \frac{V_b}{V_d}$$

This model uses empirical values of  $\eta_b = 0,7$  and  $\eta_v = 0,95$ . It is important to notice that  $\eta_b$  is the lowest of the efficiencies, which once again reminds the importance of optimizing **B** in order to improve as much as possible electron dynamics in plasma, thus increasing the discharge ion current that goes into the beam.

## Total efficiency

Total efficiency described in section 1.4 can now be calculated by substituting and rearranging its terms ( $I_b$ ,  $V_b$ ,  $\dot{m}_p$ ,  $T$ ) using the efficiencies described above. Its expression becomes:

$$\eta_t = \gamma^2 \eta_v \eta_b \eta_o \eta_m$$

The graphic shows the trend of each parameter vs the discharge voltage.

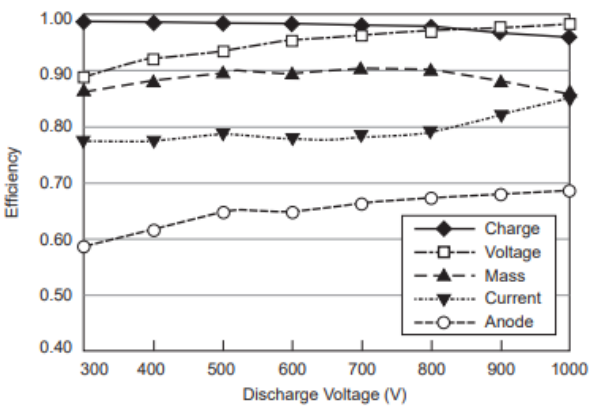
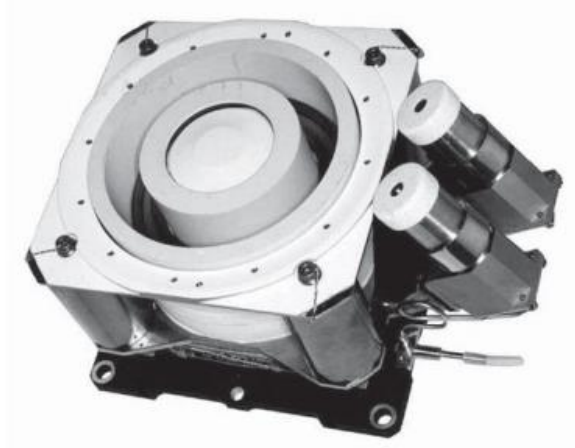


Figure 36: Efficiencies vs discharge voltage

### 3. Results and applications

This chapter presents the main results obtained with this model. It is important to remember that these results are calculated only to provide a general description of the performance of the Russian Fakel SPT-100 engine, while real data measured with sophisticated equipment may differ from these results.



*Figure 37: Picture of SPT-100 Hall Thruster*

### 3.1 Performance

First of all, it is important to list the available data of this thruster, in order to point out the missing data that can be calculated with the presented model.

Discharge voltage $V_d$ [V]	300
Discharge current $I_d$ [A]	4,5
Thrust $T$ [mN]	82
Specific impulse $I_{sp}$ [s]	1600
Propellant atomic mass (Xenon) $M$ [ $10^{-25}$ kg]	2,18

Table 8: Tabled SPT-100 data

These data are measured during a vacuum chamber test and are useful to evaluate discharge voltage and current, propellant consumption, thrust-to-power ratio, electrical efficiency, mass utilization efficiency and global efficiency, starting from the specific efficiencies described in chapter 2.4. Also, to have an idea of all types of losses, the following semi-empirical assumptions are made:

Double-to-single ion ratio ( $dts$ )	0,1
Beam semi-divergence angle $\vartheta$ [°]	20
Current efficiency $\eta_b$	0,7
Voltage efficiency $\eta_v$	0,95
Cathode efficiency $\eta_c$	0,9
Ion current toward the wall $I_{iw}$	$0,1 \cdot I_b$
Electron temperature along the wall $T_{eV,W}$ [eV]	$0,1 \cdot V_b$

Table 9: Data assumptions

Under the previous assumptions, the following results are found.

Beam voltage	$V_b = \eta_v \cdot V_d = 285 \text{ V}$
Beam current	$I_b = \eta_b \cdot I_d = 3,15 \text{ A}$
Input power	$P_{in} = V_d I_d = 1,35 \text{ kW}$
Propellant consumption	$\dot{m}_p = \frac{T\sqrt{M}}{\sqrt{2eV_b}} \cdot \frac{1}{\eta_c} = 4,44 \text{ mg/s}$
Thrust-to-Power ratio	$\frac{T}{P_{in}} = 60,74 \text{ mN/kW}$
Mass efficiency	$\eta_m = \alpha_m \cdot \frac{I_b}{e} \cdot \frac{M}{\dot{m}_p} = 0,92$
Thrust correction factor	$\gamma = \alpha_T \cdot F_T = 0,915$
Electrical efficiency	$\eta_e = \frac{P_b}{P_{in}} = 0,67$
Total efficiency	$\eta_m = \gamma^2 \eta_m \eta_e = 0,52$

Table 10: Model results

It is possible to notice that these values are close to the ones reported by the constructor, but a bit more optimistic. For example, the tabled thrust correction factor is 0,9 against the 0,915 found here because this model also considers double ionizations, but neglects multiple ionizations. Also, the total efficiency seems to be better than expected (0,52 vs 0,50 reported) because some minor loss mechanisms, such as power to generate magnetic fields, have been ignored in this computation.

### 3.2 Advantages and limitations

In this section, they will be discussed model advantages and limitations. In terms of benefits, the best aspect is the simplicity of the calculation. In fact, almost all the parameters and results are calculated using relatively simple mathematical operations, which makes it very suitable as the basis of a numerical code. Also, despite its simplicity, the model provides a wide view over all the considered phenomena, especially for the study of power loss mechanisms in the chamber. However, its limits are quite strict. First, this model largely uses semi-empirical relations, which can be very precise within the application field but completely useless outside of it. Due to this limit, the model should be almost completely re-arranged for the study, for example, of a small Hall Thruster with a power of few Watts. The main differences would be in the plasma parameters: a completely different power level would lead to different electron temperature, plasma density, ion bombardment and collisions rates, so all the relations about these phenomena should be corrected. Also, different power levels would lead to different thrusters' dimensions: in the case of small thrusters, plasma physic must be integrated with fluidodynamic's equations to have an acceptable description of plasma behaviour. Lastly, secondary phenomena such as secondary electron emission from walls, electron emission during ionization and plasma instabilities are not

considered: their integration in the model would provide a better plasma description and power loss computation, but it would require an in-depth study of plasma physics and would lead to a much more complicated model for what concerns the mathematic involved.

### **3.3 Applications**

The first application of Fakel SPT-100 thruster was in 1971 for station keeping in small satellites. Since then, about 140 Hall Thrusters have been operated in space, first by the Soviet Union and then by the Russian Space Agency. In the Western world, Hall thruster have been developed almost 30 years later, with the first launch of a HT in a spacecraft in 1998 in US (D-55 TAL thruster, designed for the demonstrative STEX mission) and in 2003 in Europe (PPS-1350-G thruster, inspired by Fakel SPT-100 for the lunar orbiting SMART-1 mission). The most valuable aspect of these thrusters is their ability to produce high thrust with a relatively small power consumption. This is possible thanks to the low voltage-high current combination in the beam, which allows for high thrust without requiring a huge power. Also, once the thruster is properly designed, its life can be extended up to few tens of thousands of hours, making it suitable for relatively long missions: this is possible thanks to the low power required, which prevents premature erosion phenomena and heat degradation. On the other hand, there are some drawbacks. Firstly, apart from thrust, Hall thrusters typically offer worse performance than ion thrusters when specific impulse, fuel consumption and global efficiency are taken as reference values. This is mostly related to the low beam voltage, which reduces the exit velocity of ions, thus reducing the specific impulse. Also, global efficiency is affected by a non-negligible double-to-single ions ratio, which reduces the mass efficiency and leads to a higher propellant consumption. Another aspect that must be considered is that, due to the interaction between the magnetic field and the ion current toward the exit, it is quite difficult to limit the beam's semi-divergence angle. This leads to the ElectroMagnetic Interactions (EMI) between thruster and spacecraft typical issues, making it more difficult to design a proper integration between the two of them. The last aspect, which affects almost all the electric thrusters, regards their global efficiency when high power levels are considered. In fact, a low efficiency produces high power loss, which is transferred to the thruster and to the spacecraft as heat. If a huge power is considered, together with a low efficiency, the thermal control system has a huge amount of heat to dissipate, which is a very critical aspect in space missions.

## 4. Bibliography and websites

[1] Casalino, L. (2022). Slides di space propulsion. Torino.

[2] Dan M. Goebel, I. K. (March 2008). Fundamentals of Electric Propulsion: Ion and Hall thrusters. Jet Propulsion Laboratory, California Institute of Technology: JPL Space Science and Technology Series.

[3] "Hall-effect Thrusters".

Available at: [https://en.wikipedia.org/wiki/Hall-effect\\_thruster](https://en.wikipedia.org/wiki/Hall-effect_thruster)

[4] <https://electricrocket.org/IEPC/IEPC-2007-142.pdf>

[5] [https://www.esa.int/ESA\\_Multimedia/Images/2004/09/SPT-100](https://www.esa.int/ESA_Multimedia/Images/2004/09/SPT-100)

[6] "PPS-1350 Thruster". Available at: <https://en.wikipedia.org/wiki/PPS-1350>

[7] [https://www.researchgate.net/figure/A-cut-out-view-of-the-3D-model-of-resistojet-thruster\\_fig2\\_329177702](https://www.researchgate.net/figure/A-cut-out-view-of-the-3D-model-of-resistojet-thruster_fig2_329177702)

[8] <https://cl.pinterest.com/pin/361062095124828639/>

[9] <https://www.eoportal.org/satellite-missions/proba-2>

[10] <https://www.satcatalog.com/component/at-1k-arcjet/>

[11] [https://ocw.mit.edu/courses/16-522-space-propulsion-spring-2015/a275de9b17e8ff642c742632a0c5f380\\_MIT16\\_522S15\\_Lecture16.pdf](https://ocw.mit.edu/courses/16-522-space-propulsion-spring-2015/a275de9b17e8ff642c742632a0c5f380_MIT16_522S15_Lecture16.pdf)

[12] <https://pepl.engin.umich.edu/pdf/AIAA-2004-3602.pdf>

[13]

[https://www.researchgate.net/publication/344912800\\_Fluid\\_modeling\\_of\\_transport\\_and\\_instabilities\\_in\\_magnetized\\_low-temperature\\_plasma\\_sources](https://www.researchgate.net/publication/344912800_Fluid_modeling_of_transport_and_instabilities_in_magnetized_low-temperature_plasma_sources)

## 5. Thanksgiving

Al termine del mio percorso universitario, ritengo sia giusto ringraziare tutti coloro che mi hanno sostenuto sino al raggiungimento di questo importante traguardo. Ringrazio mio fratello Alessio per avermi quotidianamente sopportato, e i miei genitori, che hanno fatto del loro meglio per arrivare insieme a me a questo traguardo. Nonostante i problemi, nonostante le difficoltà, nonostante tutto.

Ringrazio il resto della mia famiglia, i miei nonni e i miei Zii, che hanno sempre creduto in me. Ai loro occhi sono eternamente rimasto il 'Fabietto' valoroso di sempre, e questo mi ha aiutato a ripristinare in me la fiducia e l'autostima ogni volta che le perdevo.

Ringrazio gli amici che ci sono stati da tutta la vita, dal liceo, dall'università e dal più recente passato: con loro ho condiviso le mie paure e soprattutto ho avuto la possibilità di rimanere spensierato. Mi hanno sempre accolto col sorriso migliore, mi hanno fatto sentire normale quando credevo di 'dovermi buttare via', mi hanno regalato tante opportunità per riflettere e per crescere, per rendermi conto di ciò che sono. Ho trovato in loro un 'aggancio' verso la normalità quotidiana nei momenti più tristi e bui di questo difficile percorso, essenziale per riuscire ad arrivare fino alla fine della mia carriera universitaria.

Per ultima in questa lista, ma prima per importanza, ringrazio Giorgia, che in questi anni di fatica e malessere è stata molto più che una fidanzata. Ha saputo starmi accanto in ogni mia difficoltà, in ogni mia arresa, in ogni mio momento di rabbia e frustrazione. Ha trovato le parole giuste per riportarmi sempre verso la tranquillità, dandomi un'enorme serenità quando tutto intorno a me volgeva per il peggio. Ha sopportato con me una grande parte del peso di questi anni, non privi di gioie, ma sicuramente densi di problemi, crisi, tristezza e sconforto. Se oggi sono arrivato qui, lo devo in parte anche a lei.

Infine dedico questi anni alla mia forza e alla mia perseveranza, alla mia testardaggine, che mi hanno sempre contraddistinto anche nelle difficoltà. Sono orgoglioso di aver dimostrato per la seconda volta che non ha importanza quanto sia lunga e difficile la sfida: un IRONMAN arriva sempre fino in fondo, nonostante i dolori lungo il cammino, finché la sua mente e il suo cuore hanno voglia di farcela.